UM-HSRI-79-9

SIMULATION OF THE DIRECTIONAL RESPONSE CHARACTERISTICS OF TRACTOR-SEMITRAILER VEHICLES

MVMA Project #1.39

Final Technical Report

Motor Truck Braking and Handling Performance Study

P.S. Fancher, Jr.
C. Mallikarjunarao
R.L. Nisonger

March 1979

Highway Safety Research Institute
The University of Michigan
Ann Arbor, Michigan 48109

Technical Report Documentation Page

1. Report No.	2. Government Accession No.	3. Recipient's Catalog No.
UM-HSRI-79-9		

4. Title and Subtitle	5. Report Date
SIMULATION OF THE DIRECTIONAL RESPONSE CHARACTERISTICS OF TRACTOR-SEMITRAILER VEHICLES	March 1979
	6. Performing Organization Code
7. Author(s) P. S. Fancher, C. Mallikarjunarao, R. L. Nisonger	8. Performing Organization Report No. UM-HSRI-79-9
9. Performing Organization Name and Address Highway Safety Research Institute The University of Michigan Huron Parkway & Baxter Road Ann Arbor, Michigan 48109	10. Work Unit No. 361509 11. Contract or Grant No. MVMA Project #1.39
12. Sponsoring Agency Name and Address Motor Vehicle Manufacturers Association 300 New Center Building Detroit, Michigan 48202	13. Type of Report and Period Covered: Final 14. Sponsoring Agency Code

15. Supplementary Notes

16. Abstract

This report examines the capability of a detailed digital simulation for predicting the response to steering of tractor-semitrailer vehicles in (1) obstacle-avoidance maneuvers, (2) turning near the rollover limit, and (3) steady turning. Measured and simulated results are presented for a three-axle tractor combined with either a van-trailer or a flat-bed trailer. The influences of changes in tractor frame stiffness and/or the roll stiffness of the front suspension are considered in assessing the validity of the simulation. Particular emphasis is placed on investigating the prediction of the articulation angle existing between the tractor and the semitrailer during steady turns.

The study concludes that the simulation is capable of doing an excellent job of predicting vehicle response in obstacle-avoidance maneuvers. The simulation is found to have reasonable predictive capabilities for investigating vehicle performance in severe turning maneuvers approaching the rollover limit. (However, vehicle performance is very sensitive to steering level, forward velocity, and vehicle parameters in severe turns.) The study of the prediction of articulation angle at moderate maneuvering levels indicates that further research is needed to obtain a detailed understanding of the steady turning behavior of articulated vehicles.

17. Key Words	18. Distribution Statement
tractor-semitrailer, vehicle simulation, directional response, rollover, articulation angle, obstacle avoidance, steady turns	UNLIMITED

19. Security Classif. (of this report)	20. Security Classif. (of this page)	21. No. of Pages	22. Price
NONE	NONE	81	

TABLE OF CONTENTS

1.0 INTRODUCTION

The research investigation reported herein is part of an ongoing study of motor truck braking and handling being conducted by The University of Michigan's Highway Safety Research Institute for the Motor Vehicle Manufacturers Association of America [1]. In this ongoing study, large-scale computer-based models for simulating the braking and directional response of commercial vehicles have been developed [2,3,4]. This report addresses the capability of a detailed digital simulation (which is an extension of the model described in Reference [4]) for predicting the response to steering of tractor-semitrailer vehicles in obstacle-avoidance (lane-change), step-steer, and steady-turning maneuvers.

Previous "validation" studies have been directed at (1) using the computer models to study the braking performance of commercial vehicles equipped with antilock braking systems [5,6] and (2) assessing the ability of the computer programs to predict the directional response of straight trucks [7]. The investigation presented in this report extends the work on straight trucks by considering the influences of the articulation joint at the fifth wheel of a tractor-semitrailer vehicle.

After studying the simulation of braking and steering maneuvers separately, future validation efforts in the ongoing research program will be concerned with vehicle maneuvers involving combined steering and braking activity. Accordingly, the research described herein is a single step in a process of improving and perfecting the vehicle models.

The basic objective of this report is to compare simulated directional response with test results in order to demonstrate the strengths and weaknesses of the computer model at this stage of its development.

The main body of this report contains (1) concise sections describing the vehicles tested and the simulation employed, (2) a comparison of simulated and measured results, and (3) concluding remarks indicating the types of vehicle maneuvers that can be predicted well and recommending further research into the modeling of (a) steering systems, (b) the roll motions of tractors and semitrailers, and (c) factors influencing steady-state response.

Technical matters pertinent to the simulation of the directional response to steering of tractor-semitrailer vehicles are presented in several appendices.

2.0 DESCRIPTIONS OF THE VEHICLES USED IN THE VALIDATION STUDY

The tractor-trailer combinations which were studied are specified below:

	Tractor	Trailer
1)	International Harvester Model COF 4000D	Fruehauf Van Model FG8-F2-45'
2)	Same as (1)	Trailmobile Flat Bed Model P31TOSAH

The more important parameters affecting the directional and roll responses of the tractor, the van trailer, and the flat-bed trailer are given in Tables 1, 2, and 3, respectively. A detailed listing of the parameters of the tractor-van trailer combination is given in Appendix A.

The following tires were mounted on the indicated units:

Tractor - 10.00 x 22F Firestone Rib
Van Trailer - 10.00 x 20F Freuhauf Rib
Flat-Bed Trailer - 10.00 x 20F Firestone Rib

Lateral force and aligning moment characteristics for these tires were measured on the HSRI flat-bed tire tester. These data are presented in Appendix B.

The proper load distributions for the trailers, in their fully-loaded configuration, were obtained by rigidly attaching cast steel weights to the floor of the van or that of the flat-bed trailer; the height of the center of gravity of the payload was 13 1/2" above floor level.

In its baseline configuration, the tractor has a very torsionally compliant frame and a front suspension roll stiffness which is low compared to the roll stiffness of the rear tandem axle (see Table 1). This rear-biased roll moment distribution causes a relatively large side-to-side load transfer to take place at the rear axle of the tractor.

Table 1. Vehicle Description - I.H.C. Tractor.

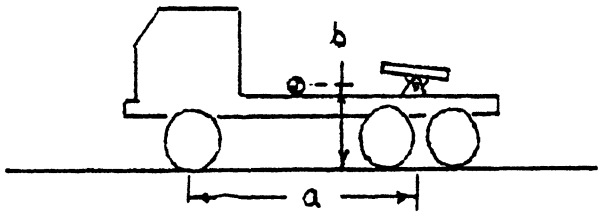

Wheelbase 'a' (in)	142
Height of c.g. above ground 'b' (in)	39
Weight of tractor (lb)	16,016
Yaw M.I. of tractor (lb.in.sec^2)	192,915
Roll M.I. of tractor (lb.in.sec^2)	18,166
Roll stiffness of front suspension (in-lb/deg)	13,385
Roll stiffness of front tandem (in-lb/deg)	16,035
Roll stiffness of rear tandem (in-lb/deg)	94,035
Frame stiffness (in-lb/deg)	20,000

All Tires - 10 x 22F Firestone Transport 1

Table 2. Vehicle Description - Fruehauf Van Trailer.

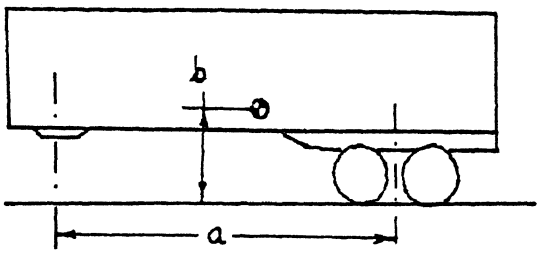

Distance 'a' (in)	410
Height of empty van sprung mass c.g. 'b' (in)	57.3
Weight of empty van (lb)	17,321
Weight of payload used during experiments (lb)	40,600
Yaw M.I. of empty van ($lb.in.sec^2$)	10.5×10^5
Yaw M.I. of payload ($lb.in.sec^2$)	17.3×10^5
Height of payload mass center above ground level (in)	64.5
Roll stiffness of each tandem suspension (in-lb/deg)	120,814
Stiffness of van structure in roll (in-lb/deg)	750,000

All Tires on Tandem Axles - 10 x 20F Fruehauf

Table 3. Vehicle Description - Trailmobile Flat-Bed Trailer.

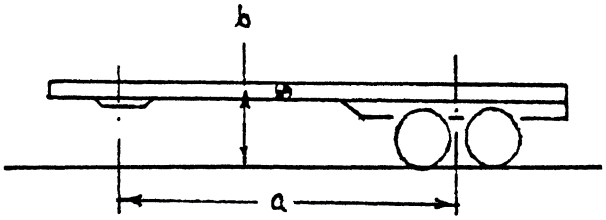

Distance 'a' (in)	408
Height of empty flat-bed sprung mass c.g. 'b' (in)	44.5
Weight of empty flat-bed trailer (lb)	13,491
Weight of payload used during experiments (lb)	42,180
Yaw M.I. of empty flat-bed (lb.in.sec^2)	623,119
Yaw M.I. of payload (lb.in.sec^2)	14.25 x 10^5
Height of payload mass center above ground level (in)	67.5
Roll stiffness of each tandem suspension (in-lb/deg)	56,000
Stiffness of flat-bed structure in roll (in-lb/deg)	12,000

All Tires on Tandem Axles 10 x 20F Firestone Transport 1

The validity of the model in simulating the directional response of a tractor-trailer combination was also studied for the case in which the tractor has a roll moment distribution (between front and rear axles) which is significantly different from that of the baseline tractor. This change was achieved by increasing the stiffness of the tractor frame and the roll stiffness of the front suspension by externally attaching a stiffener to the frame and a front suspension roll stabilizer bar, respectively. The roll stabilizer bar and frame stiffener used in these experiments are pictured in Figure 1.

The values of the roll stiffness of the front suspension and the torsional stiffness of the frame, as measured for the baseline and modified configurations, are as follows:

Tractor front suspension roll stiffness (in-lb/deg)	
baseline	13,385
with roll bar	113,385
Torsional stiffness of tractor frame (in-lb/deg)	
baseline	20,000
with frame stiffener	120,000

Test results showing the influence of various combinations of trailer, trailer loading, tractor frame stiffening, and additional front roll stiffness are presented in Section 4.0.

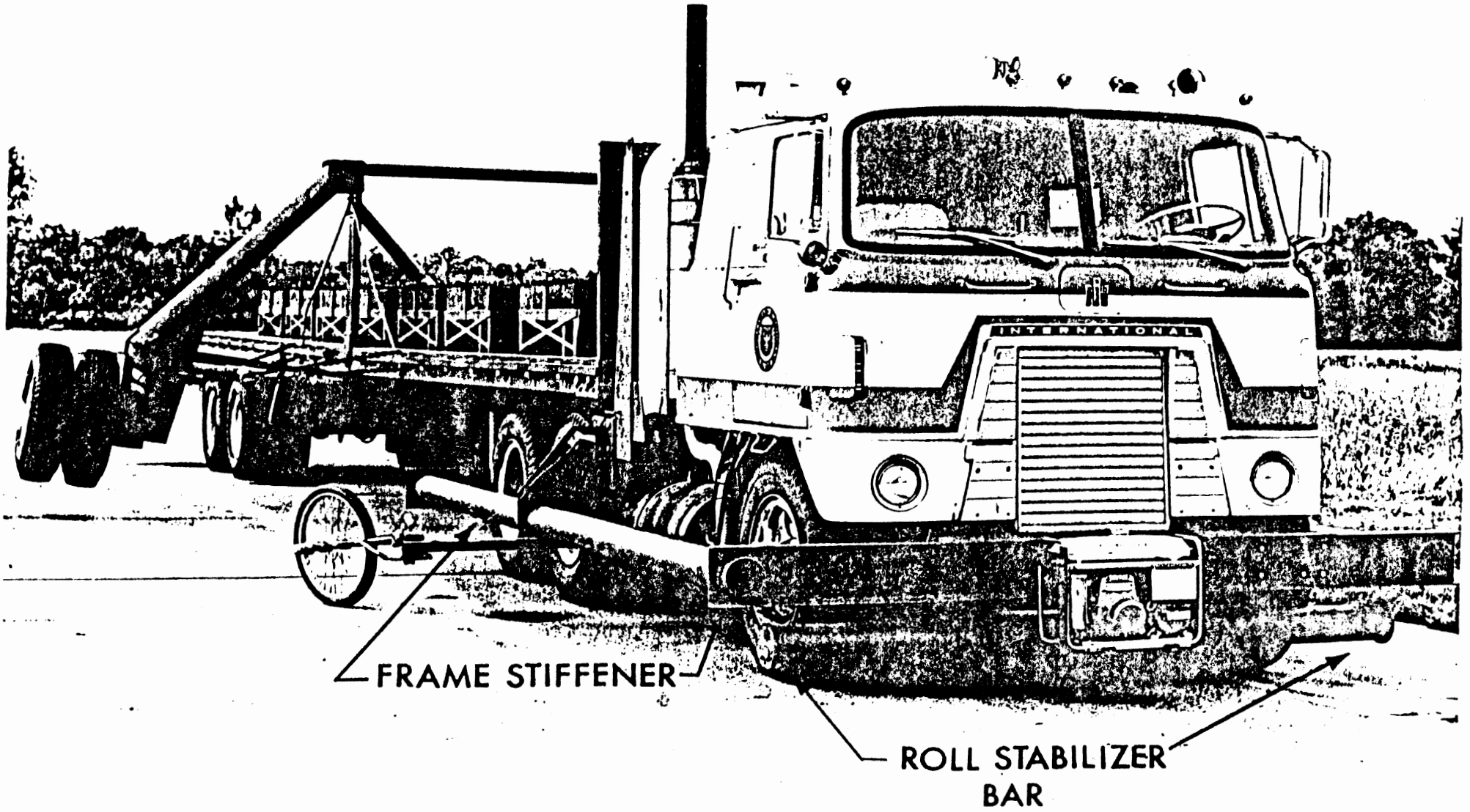

Figure 1. "Frame-stiffened" and "roll-stabilized" test vehicle.

3.0 FEATURES OF THE PHASE II DIRECTIONAL RESPONSE SIMULATION

The Phase II simulation consists of a comprehensive mathematical model capable of predicting the response of a commercial vehicle to steering and/or braking inputs. The degrees of freedom used in modeling a tractor-semitrailer vehicle include: (1) roll, pitch, and yaw rotation and longitudinal, lateral, and bounce translation of the tractor's sprung mass, (2) six analogous degrees of freedom for the semitrailer's sprung mass, (3) a roll and a bounce degree of freedom for each single-axle suspension, (4) bounce, pitch, and roll motions of each set of tandem axles, and (5) a rotational degree of freedom for each single or dual wheel. However, it should be noted that, although the model used to simulate a five-axle tractor-semitrailer vehicle has 32 degrees of freedom (as required to simulate combined braking and turning maneuvers), only 11 degrees of freedom (lateral, yaw, and roll motions of the tractor and semitrailer sprung masses and roll motions of the five axles) are important in this study of directional response without braking.

For the study of the directional response to steering, the main assumptions made in developing the Phase II model are as follows:

1) The fifth wheel can be treated as a "stiff" spring-damper system which keeps the tractor and trailer closely tied together.

2) The fifth wheel transmits a roll moment between the tractor and the semitrailer. The magnitude of the moment at the fifth wheel depends upon tractor and semitrailer roll angles and roll rates.

3) Each suspension has a "roll center" at which the forces of constraint between the sprung and unsprung masses act.

4) Estimates of the lateral acceleration of unsprung masses can be used in computing the "forces of constraint" between the sprung and unsprung masses. (See Appendix C.)

5) Steering system dynamics are neglected. Nonetheless, a number of options for treating roll steer, steering compliance, and side-to-side differences in front-wheel steer angles exist in the simulation.

The simulation features (1) a detailed tire model, (2) a means for representing large amounts of coulomb friction in the suspensions, (3) options for treating the dynamics of different types of tandem suspensions, and (4) provisions for including the influences of torsional compliances in the tractor and semitrailer frame structures. A comprehensive discussion of the Phase II model is given in Reference [4]. Pertinent details of the basic form of the equations programmed into the simulation are presented in Appendices C and D. The semi-empirical tire model, which can be used to accurately fit measured tire data, is thoroughly discussed in Reference [8].

4.0 COMPARISONS OF SIMULATED AND MEASURED DIRECTIONAL RESPONSE

4.1 Lane-Change-Type Transient Maneuvers

This section presents time histories indicating that the simulation does an excellent job of predicting directional response to steering in aggressive obstacle-avoidance maneuvers.

To obtain valid predictions of directional response, it is clearly necessary to have accurate representations of the steer angles of the front wheels. Accordingly, the angular positions of the steering wheel and the left- and right-front wheels were recorded during lane-change maneuvers. A cut-away view of the front-wheel angle measuring device used in this validation study is shown in Figure 2. This device directly measures the orientation of both left and right wheels with respect to the tractor body and hence eliminates the need for applying a roll-steer correction in the calculation. (Note: this correction would be needed if the front-wheel angles were measured with respect to the front axle.) Samples of typical time histories of steering-wheel, left-wheel, and right-wheel angles during a lane-change maneuver are shown in Figure 3.

It should be noted that the front-wheel angles are functions of not only steering-wheel angle, but they are also influenced by response variables such as roll angle, aligning torque at the front wheels, etc. Ideally, the steering input to the simulation should be steering-wheel angle, with all other factors influencing the orientation of the front wheels being properly accounted for in the model of the steering system. Nevertheless, time histories of the front-wheel angles were used as inputs in this validation study, thereby allowing the examination of directional response without the confounding difficulties of including detailed steering system properties in the calculations. (An ongoing project is addressing the properties of truck steering systems.)

A typical example showing excellent agreement between simulated and measured results is presented in Figure 4. Figure 4 shows the

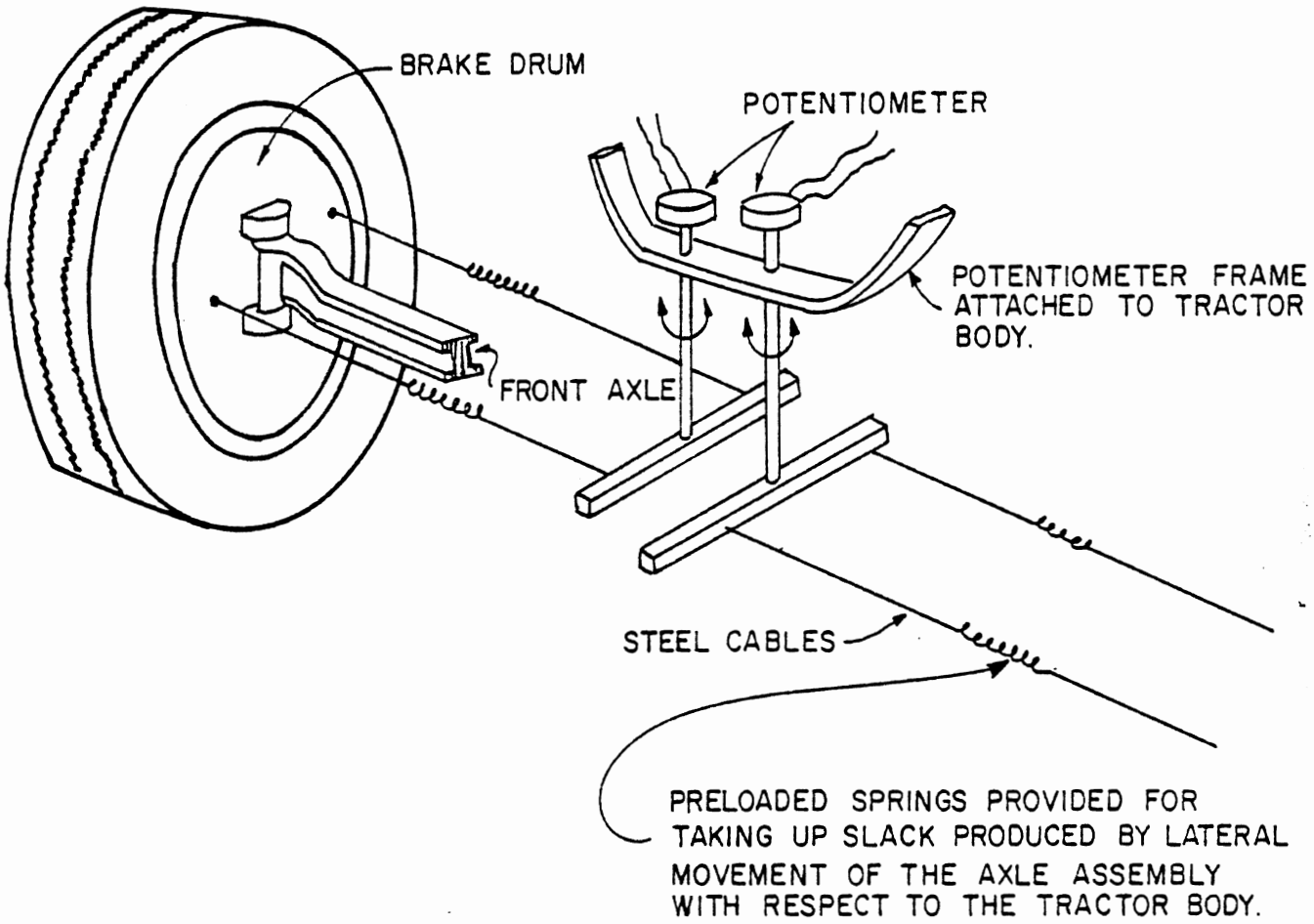

Figure 2. Cutaway view of the device used for measuring left and right front-wheel angles.

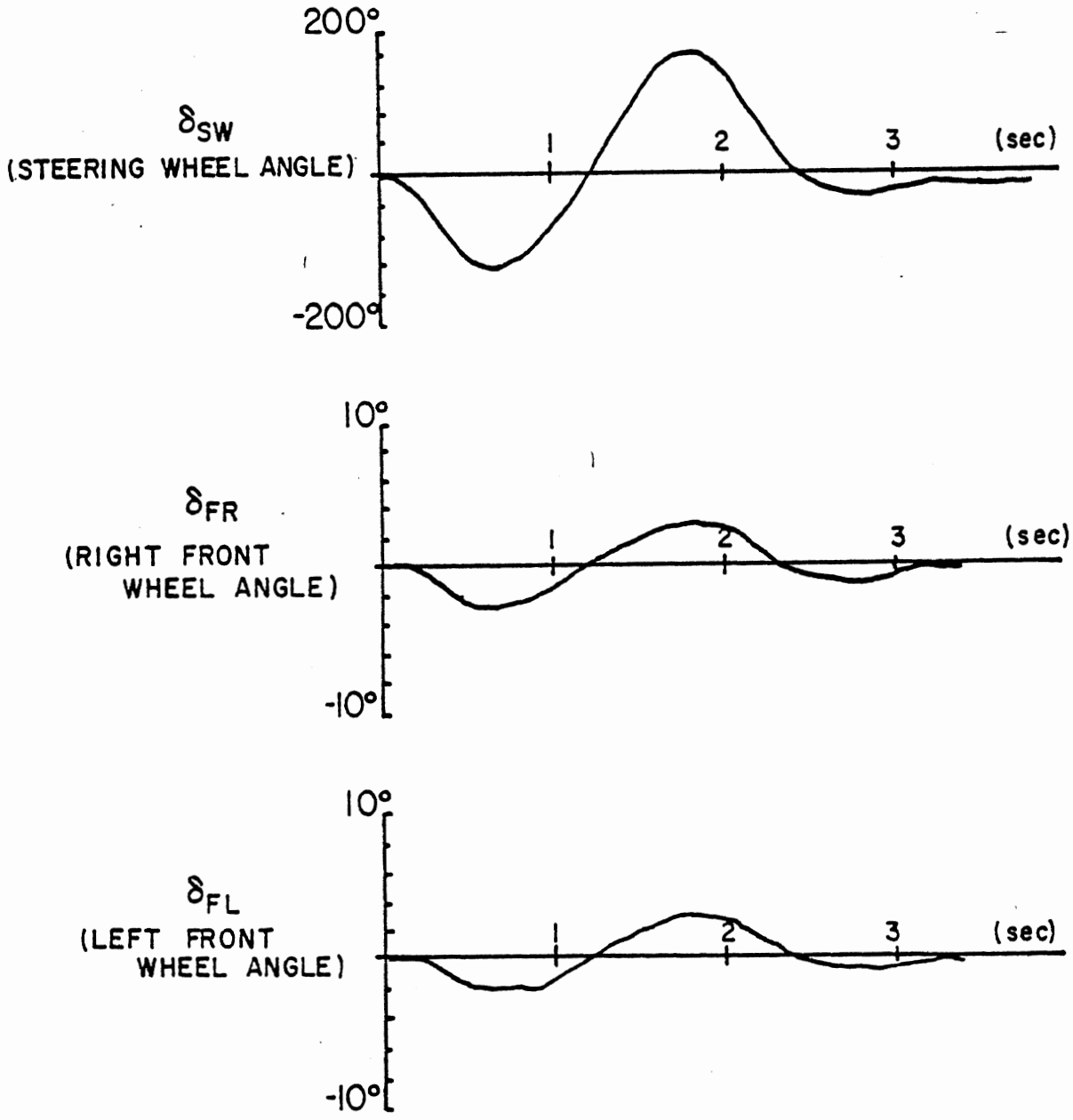

Figure 3. Typical time histories of steering-wheel, right-wheel, and left-wheel angles during a lane-change maneuver.

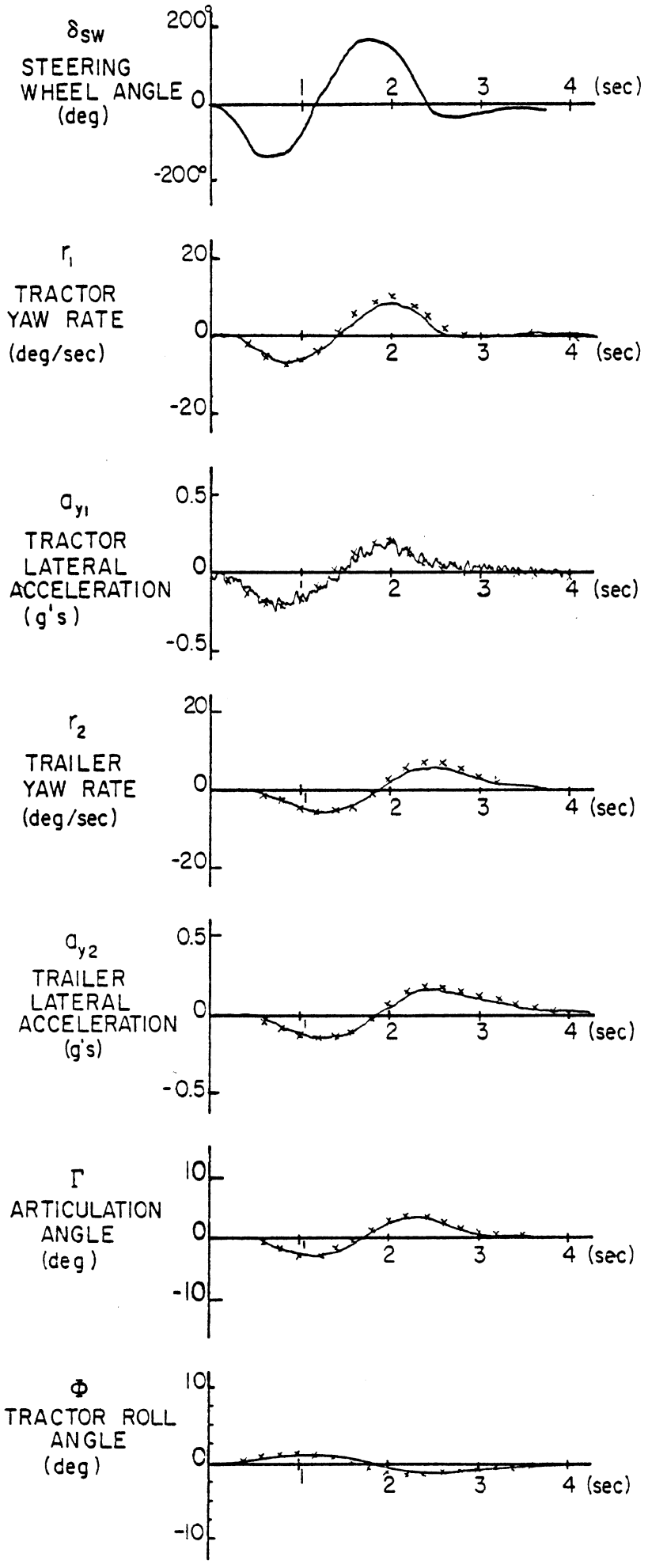

Figure 4. Response of a tractor-loaded van trailer combination at a speed of 43 mph.

response of the tractor/loaded van trailer combination to a 2.5-second lane-change maneuver resulting in a peak lateral acceleration of 0.2 g. The simulated response (predicted from measured front-wheel angles) coincides almost perfectly with measured time histories of articulation angle, tractor yaw rate and lateral acceleration, trailer yaw rate and lateral acceleration, and tractor roll angle.

In contrast to the loaded situation, if the trailer is empty, the tires on the tractor rear axles and the trailer axles operate at much smaller vertical loads; moreover, the side-to-side vertical load transfers that take place during rapid maneuvering of the vehicle are of much smaller magnitude. The influences of the changes in tire and vehicle characteristics brought about by going from a loaded to an empty condition are adequately represented in the model as evidenced by the very favorable correspondence between test data and simulated results shown in Figure 5.

Further evidence of the general validity of the simulation is presented in Figure 6, which contains results for a tractor/loaded flat-bed trailer combination. The flat-bed trailer used in this experiment has a very torsionally compliant frame and a suspension which is only half as stiff as the van trailer's suspension (see Tables 2 and 3). Again, the simulated results compare well with the test data.

In summary, the mathematical representation of the tractor-semitrailer vehicle (described in [4,8] and Appendices C and D) is sophisticated enough to make accurate predictions of the transient response of the vehicle in lane-change or obstacle-avoidance maneuvers.

4.2 Constant Steer Turns Near the Rollover Limit

Comparisons of test data with simulated performance for step-steer maneuvers at or near the "wheel lift-off" condition reveal the model's ability to predict limit behavior (such as yaw divergence and/or rollover) of the vehicle.

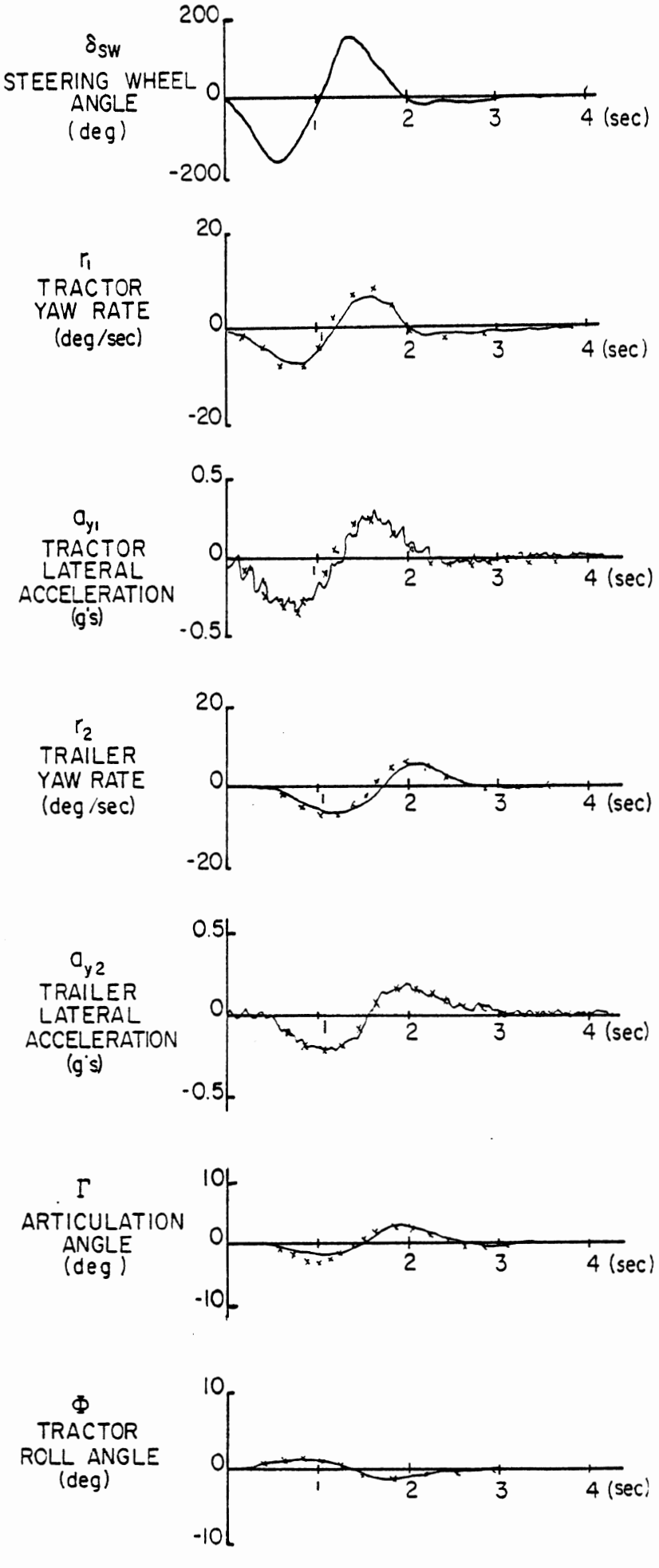

Figure 5. Response of a tractor-empty van trailer combination at a speed of 50 mph.

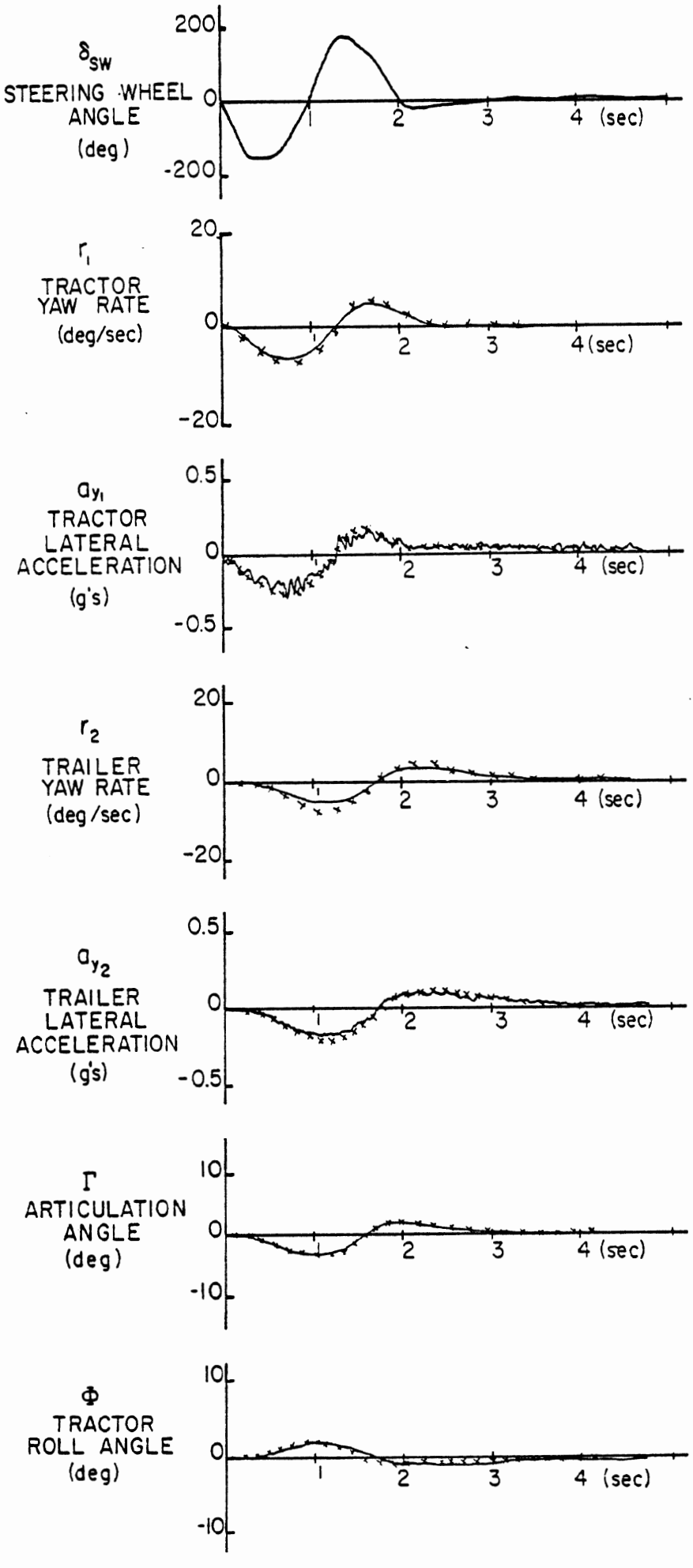

Figure 6. Response of a tractor-loaded flat-bed trailer combination at a speed of 45 mph.

In this maneuver, starting with the vehicle traveling in a straight-ahead direction, a steering input, similar to that shown below, is generated by the driver and the ensuing motion is recorded.

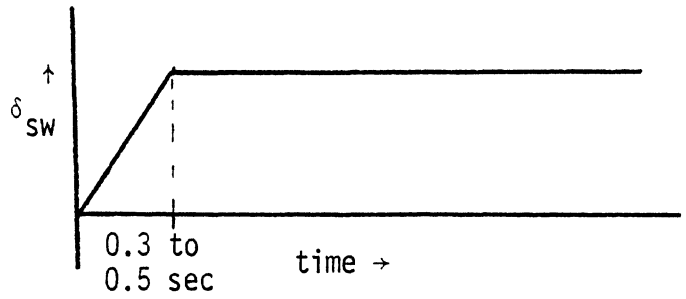

By experimenting with the test vehicle at a selected velocity, it is possible to find a level of steering input which produces a vehicle response on the verge of (1) wheel lift-off or (2) touch-down of the outriggers. (Note: outriggers were fitted to the trailer to prevent rollover.)

During the set of limit-maneuver experiments, the presence of the roll stabilizer bar on the front axle of the tractor (see Figure 1) prevented the mounting of the front-wheel angle measuring device, thereby necessitating the extrapolation of front-wheel angle data obtained during other constant steer maneuvers conducted in the same speed range but at lower lateral acceleration levels.

The magnitude of the steady-state values of left- and right-wheel angles measured during a series of step-steer experiments (at 45 mph) are plotted on the ordinates of Figures 7 and 8, respectively, with the corresponding magnitudes of steering-wheel angle being plotted on the abscissas of these figures. "Straight-line fits" to these data indicate "apparent" ratios of steering-wheel angle to the left- and right-front wheel angles of 70 and 76, respectively. (These apparent ratios are approximately twice as much as the geometric ratio of 37 that was measured for this steering system with no externally applied steering torque.)

Estimates of front-wheel angles based on the apparent steering ratios have been used in this study for simulating vehicle performance near the rollover limit.

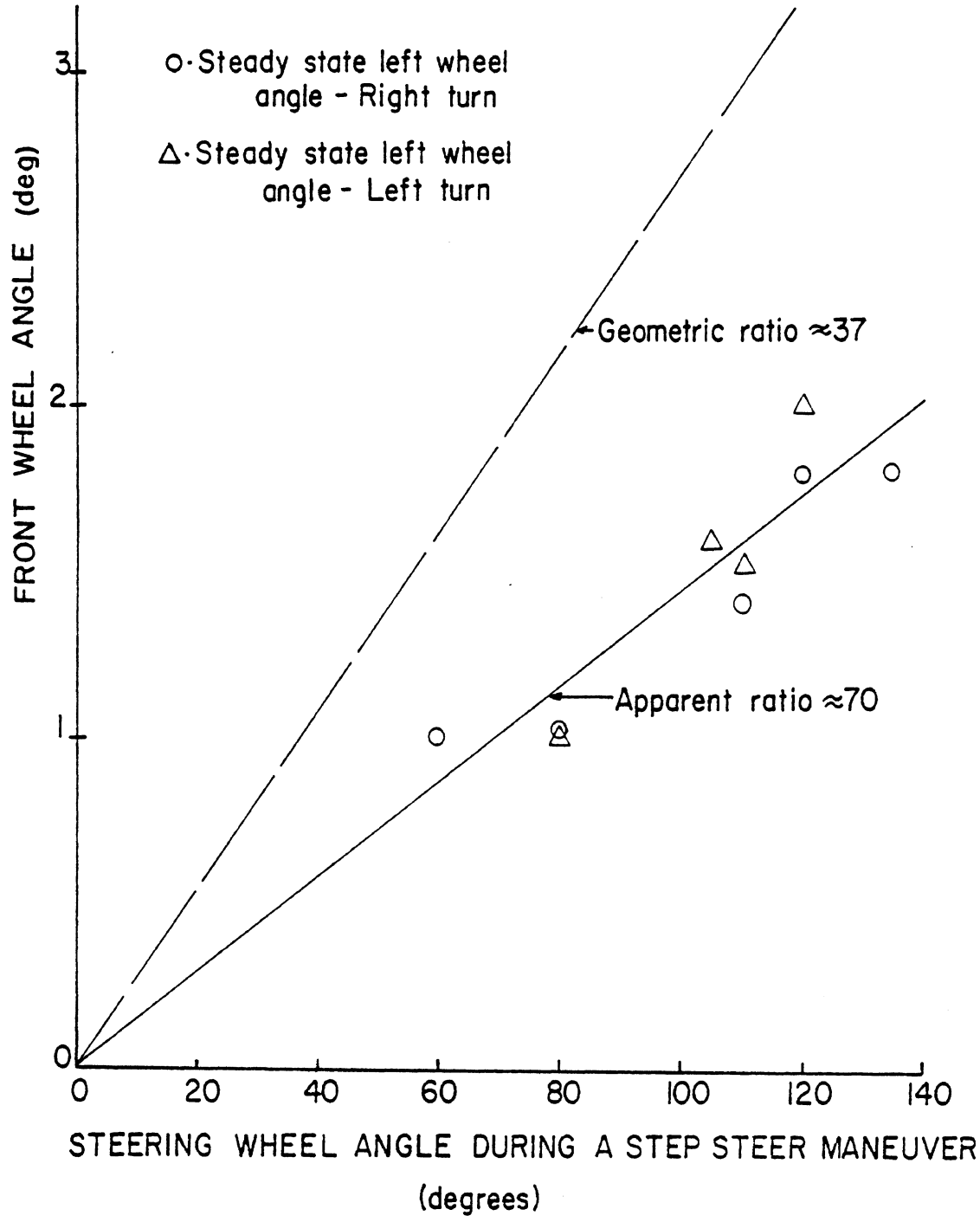

Figure 7. Relationship between the left front-wheel angle and the steering-wheel angle during steady turns.

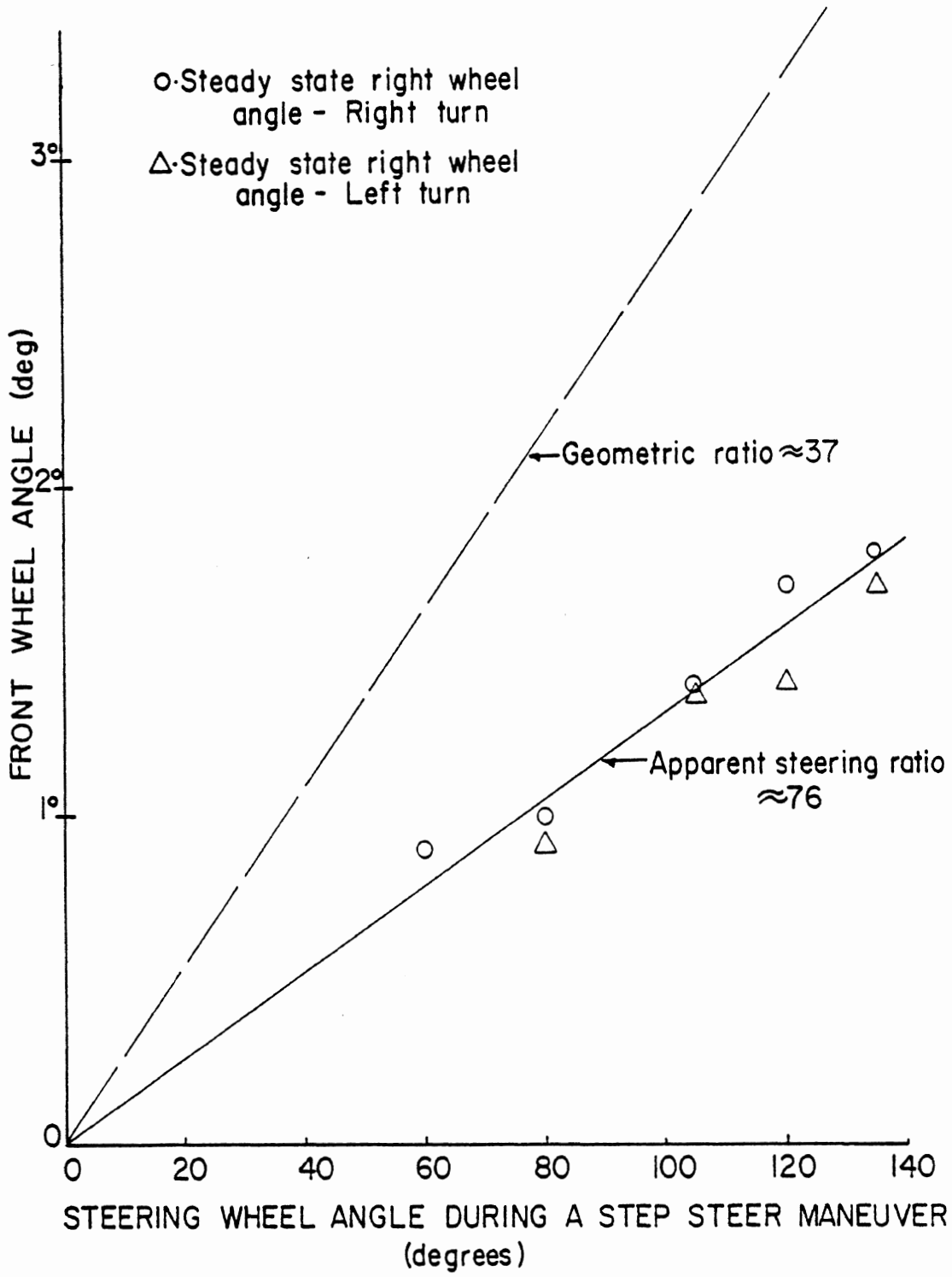

Figure 8. Relationship between the right front-wheel angle and the steering-wheel angle during steady turns.

Figure 9 illustrates several interesting points concerning vehicle performance and the prediction of vehicle performance at or near the rollover limit. First, in a severe step-steer maneuver (exceeding 0.5 g, as shown in Figure 9) the vehicle responds quickly in the beginning of the maneuver, reaching relatively high levels of lateral acceleration in approximately 2 seconds for the tractor and 2.5 seconds for the trailer. After the initial period of rapid response, the motion variables (i.e., yaw rates and lateral accelerations) gradually increase until the condition for wheel lift-off and possibly rollover occur. The instant at which wheels lift off depends upon (1) the forward velocity at which the maneuver is performed and (2) the level of steering input used. For example, as illustrated by the simulated results, wheel lift-off might have occurred anytime between 3 and 6 seconds after the initiation of the steering input.

If precisely appropriate levels of forward velocity and steering input are used in the simulation, an excellent agreement between simulated and measured results can be attained. However, as illustrated in Figure 9, a 5% change in steering angle or a 2-mph change in velocity can have a large influence on the time of wheel lift-off and the initiation of a divergent roll response.

With regard to the rollover of vehicles in actual service, the results shown in Figure 9 indicate that there is a threshold value of lateral acceleration (and roll angle) above which a vehicle will roll over. By carefully modulating the forward velocity and the steer angle, a skillful driver may be able to maintain a vehicle on the verge of rollover for several seconds, but a small error in speed or steering can cause rollover to proceed rapidly.

It should be noted that the simulation is not designed to be an accurate model of vehicle motion once rollover has started. Whether the simulated results are representative of the end of a rollover cannot be determined from the test results because the vehicles were equipped with outriggers. Nevertheless, the results indicate that the model is capable of predicting wheel lift-off and the onset of rollover.

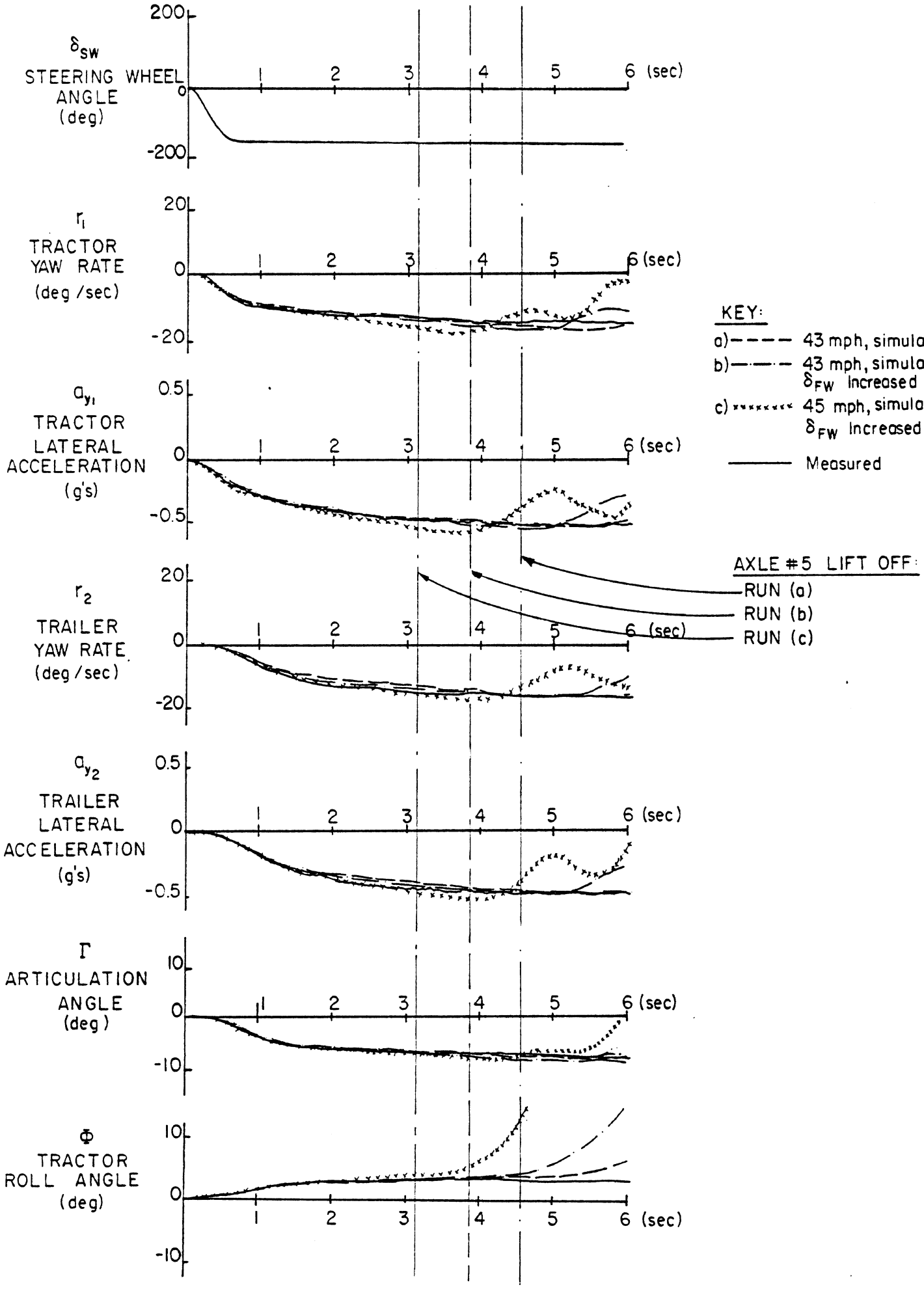

Figure 9. Response of a tractor (baseline)-loaded van trailer combination during a severe step-steer maneuver.

In addition to studying baseline vehicle performance, it is of interest to examine the model's utility in predicting changes in roll or directional response caused by changes in the distribution of side-to-side load transfer. Even though the frame stiffener and roll stabilizer bar employed to achieve changes in roll moment distribution would never be used in practice (see Figure 1), they do provide changes in vehicle characteristics suitable for studying the influence of altering the roll moment distribution and for evaluating the ability of the simulation to predict these influences. The results emphasized here pertain to demonstrating the simulation's capabilities. (An NHTSA study [10] is addressing the influence of frame compliance and roll stiffness distribution on yaw divergence and rollover.)

A comparison of the time histories presented in Figures 9 and 10 indicates that response of the vehicle when the roll stabilizer and frame stiffener are employed is significantly different from the response of the baseline vehicle. In the case of the vehicle with a front roll stabilizer bar and a frame stiffener, the tractor achieves nearly 0.5 g of lateral acceleration in approximately 2 seconds after the initiation of steering; however, in contrast to the baseline vehicle, the lateral acceleration of the modified vehicle does not continue to increase after the initial rapid response to the steering input. The simulated response, superimposed upon the test data plotted in Figure 10, is in reasonable agreement with the measured results, thereby illustrating the adequacy of the model for investigating the influence of changes in roll moment distribution.

In addition to a change in the character of the transient response, the vehicle with the tractor frame and front suspension stiffened was found to require a 54% higher steering input to attain approximately the same yaw rate and lateral acceleration levels as the baseline vehicle in severe turning maneuvers. The computed results indicate a similar decrease in yaw rate gain.

Possibly better agreement between simulated and measured results could be obtained if the front-wheel angles were measured and used in

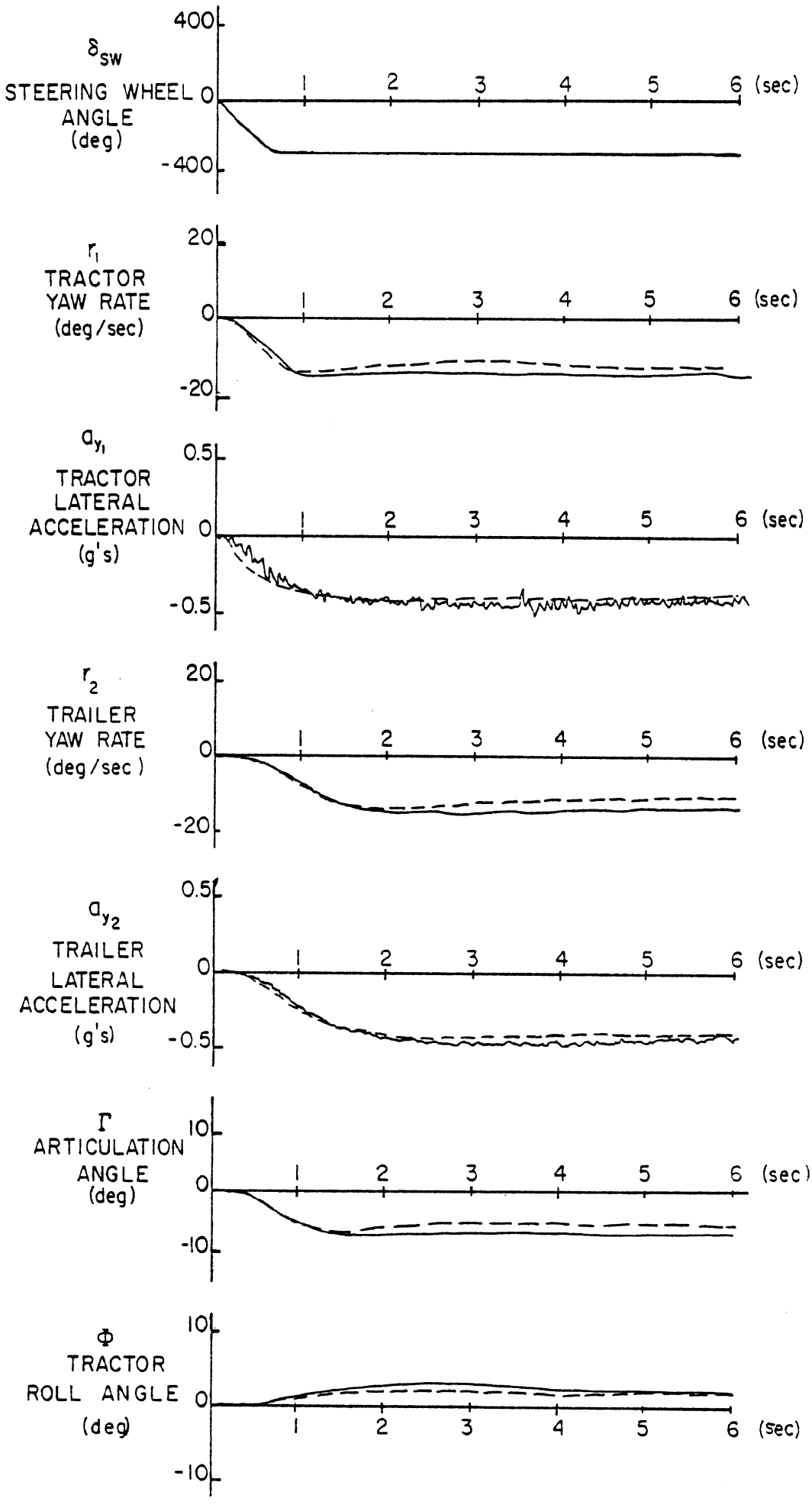

—— MEASURED – – – SIMULATED

Figure 10. Response of a tractor (with roll stabilizer bar and frame stiffener)-loaded van trailer combination during a severe step-steer maneuver at 45 mph.

the calculations. Better than that, the comprehensiveness of the simulation could be improved by including steering-system properties in the calculations.

It should be noted, though, that, as in the baseline situation, vehicle performance near the rollover limit is very sensitive to forward velocity, steering level, and critical vehicle parameters. Excellent agreement between simulation and test can only be achieved if great care is exercised in determining velocity, front-wheel angles, tire properties, and roll moment distribution. The agreement achieved in the cases presented herein is believed to be reasonable, given the sensitivity of the results to input and vehicle parameters.

As discussed in Appendix D, compliance in the tractor frame is accounted for in the Phase II model by considering the tractor sprung mass as a rigid body connected to the fifth wheel by a torsional spring (the torsional compliance of the entire frame being accounted for in this spring). The roll angle of the tractor sprung mass as computed in the simulation is therefore, in effect, the roll angle at the front end of the frame.

For a situation in which the frame is relatively compliant and the front suspension is relatively stiff in roll, the approximation of treating the tractor sprung mass as a rigid body can lead to an apparent discrepancy between measured and simulated roll angle, as illustrated in Figure 11. In the experiment, the transducer measuring tractor roll angle was located in the vicinity of the tractor c.g. Since the torsional stiffness between the c.g. and the fifth wheel was relatively large for this vehicle, the measured roll angle was, in effect, the roll angle at the fifth wheel. In the situation illustrated in Figure 11 a relatively compliant frame section (between the c.g. and the front suspension) is in "series" with a stiff front suspension, which condition results in a small roll angle at the front end of the tractor as compared to the roll angle at the fifth wheel. Hence, the computed roll angle is found to be considerably less than the measured roll angle in Figure 11.

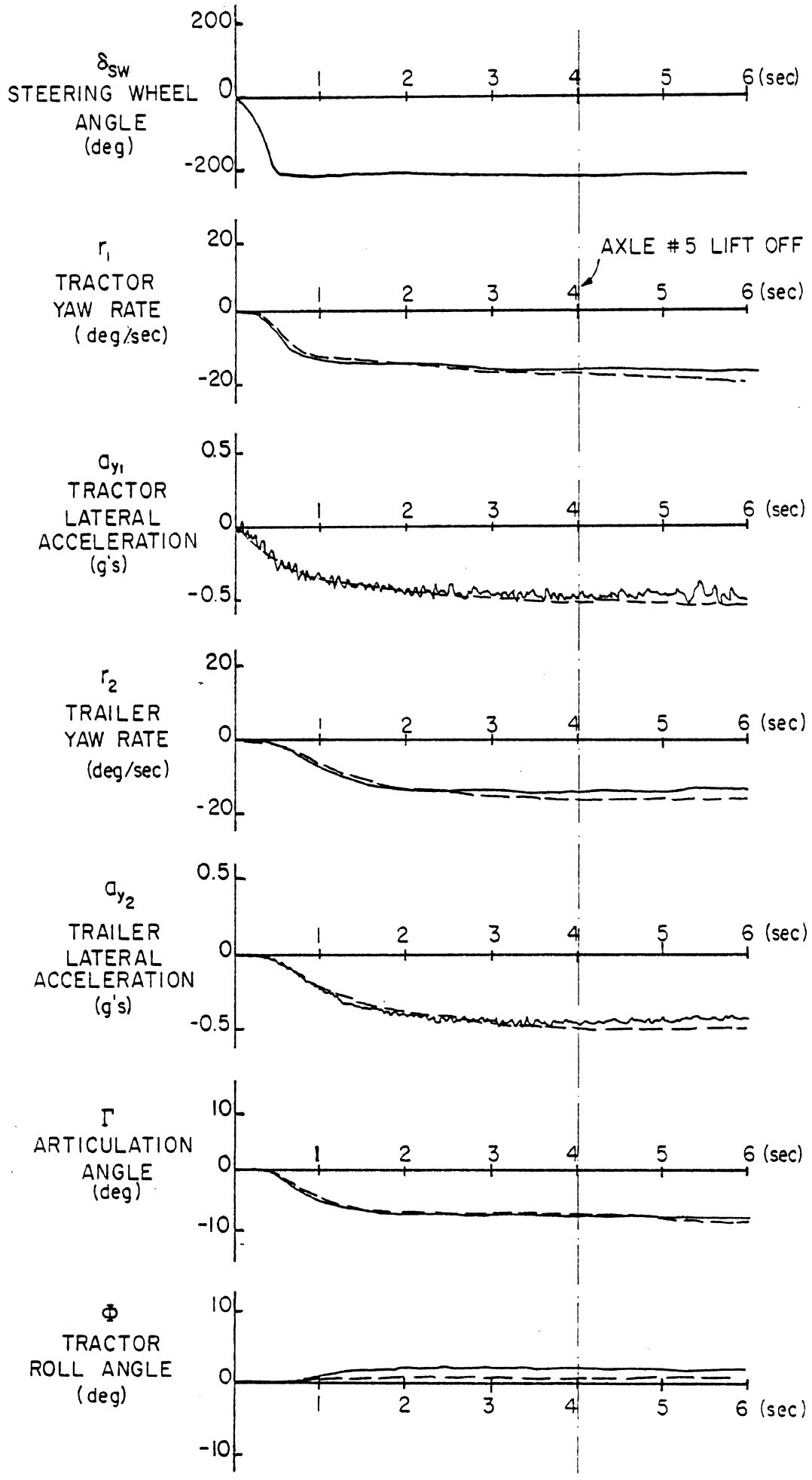

——— MEASURED ---- SIMULATED

Figure 11. Response of a tractor (with roll stabilizer bar)-loaded van trailer during a severe step-steer maneuver at 43 mph.

The results presented in Figure 11 are simply a straightforward example showing that using the Phase II program to study the influence of frame compliance on roll motion can be "tricky" and the user of the program can easily be misled if the results are not interpreted critically with considerable caution.*

4.3 Steady-Turn Articulation Angle

In addition to time history comparisons of transient results, examination of articulation angle data from steady-turning maneuvers was investigated because articulation angle is the main response variable distinguishing the directional performance of a tractor-semitrailer vehicle from that of a straight truck. (Also, the prediction of the directional performance of a straight truck was studied previously [11].) Accordingly, a special steady-state analysis was performed to aid in understanding and interpreting articulation angle results from either vehicle tests or simulations of steady-turning situations.

The results of the analysis, which is presented in Appendix E, indicate that articulation angle may be predicted by a simple function of velocity, yaw rate, axle location, load distribution, and tire properties, viz.:

$$\Gamma = \frac{\ell_2 r}{V} + K_2 rV \qquad (1)$$

where

Γ = the articulation angle

r = the yaw rate of the tractor

V = the forward velocity

---

*Clearly, this is appropriate advice concerning the interpretation of results from any model.

and ℓ_2 and K_2 are vehicle descriptors which will be defined next. The quantity ℓ_2 represents the "effective wheelbase" between the tractor rear axles and the trailer rear axles. (It is called the effective wheelbase because for tandem suspensions it is approximately, but not exactly, equal to the longitudinal distance between the lateral centerlines of the tractor rear suspension and the trailer suspension.) The quantity K_2 is defined as the "trailer understeer/oversteer coefficient" and it is related to (1) the loads on the tractor rear tires and the trailer tires and (2) the cornering stiffnesses of the installed tires. To a first approximation, the quantity K_2 is given by the following equation:

$$K_2 = \frac{F_{z_2}}{C_{\alpha_2}} - \frac{F_{z_3}}{C_{\alpha_3}} \qquad (2)$$

where

F_{z_2} is the total vertical load carried by all the tires on the tractor rear suspension

F_{z_3} is the total vertical load carried by all the tire on the trailer suspension

C_{α_2} is the total cornering stiffness for all the tires on the tractor rear suspension

C_{α_3} is the total cornering stiffness for all the trailer tires

Measured data from steady-turning tests of the three-axle tractor and the van-semitrailer are given in Table 4. Using an equation of the form

$$\Gamma_{(\text{degrees})} = \ell_2\left(\frac{r}{V}\right) + K_2 \frac{rV}{57.3g}$$

to match the data given in Table 4 yields "best fit values" (that is, values which minimize the sum of the squared errors at each data point) of ℓ_2 = 34.5 feet and K_2 = 2.6 deg/g, with an rms difference between

Table 4. Steady-Turn Articulation Angles.

	Target Velocity (mph)	Measured Values: V, Velocity (ft/sec)	r, Yaw Rate (deg/sec)	Γ, Articulation Angle (deg)
Left Turns	40	57.3	8.4	5.7
	34	51.3	7.4	5.7
	28	41.1	6.7	6.1
	22	30.8	4.9	5.7
	16	23.5	4.2	6.1
Right Turns	40	57.2	8.6	5.7
	34	48.4	7.7	5.9
	28	41.1	6.7	6.0
	22	30.8	5.3	6.4
	16	23.5	4.7	7.0

measured and fitted articulation angle of 0.1 degree. Similar values of ℓ_2 and K_2 determined from runs of the full-scale simulation are as follows: ℓ_2 = 34.3 ft. and K_2 = -1.3 deg/g. Figure 12 provides a graphical illustration of these results.

For this vehicle, the distance between the center of the tractor rear suspension and the center of the trailer suspension is 410 in., or 34.2 ft., indicating that the values of effective wheelbase, ℓ_2, determined from either simulation or test are reasonable.

Based on the tire data and the vehicle loading information given in Appendix A, the loading and cornering stiffness values needed for predicting K_2 using Equation (2) are as follows: F_{z_2} = 31,400 lbs., F_{z_3} = 33,600 lbs., C_{α_2} = 5,450 lbs/deg, and C_{α_3} = 4,900 lbs/deg. The predicted value of K_2 obtained from Equation (2) is -1.1 deg/g. The value of K_2 predicted by the simplified model of Appendix E is approximately equal to the value of K_2 determined from the simulated tests.

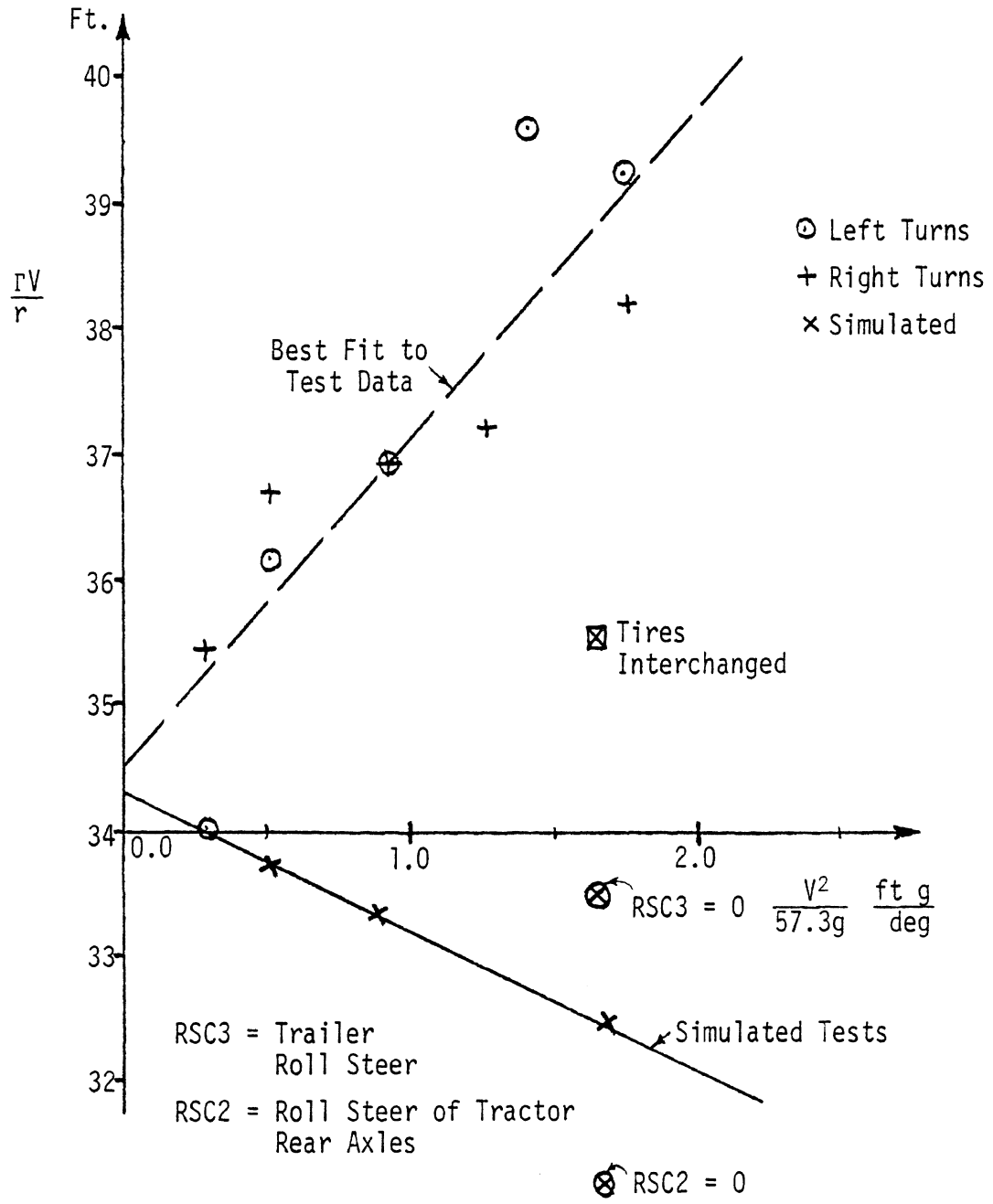

For a steady turn,

$$\Gamma = \frac{\ell_2 r}{V} + \frac{K_2 V r}{57.3g}$$

or

$$\frac{\Gamma V}{r} = \ell_2 + \frac{K_2 V^2}{57.3g}$$

Figure 12. Steady turn results.

To study possible causes for the difference between simulated and measured performance in steady-turning maneuvers, three parametric changes were simulated and the calculated results are superimposed on Figure 12. The three parametric changes were (1) setting the roll steer of the tractor rear axles to zero (RSC2=0), (2) setting the roll steer of the trailer axles to zero (RSC3=0), and (3) interchanging the tires on the trailer with those on the rear axle of the tractor. As seen by inspecting the results shown in Figure 12, the influence of the roll steer changes are nearly equal in magnitude but of opposite polarity. As anticipated, reversing the tires between the tractor and the trailer changed the results at 40 mph to be consistent with an understeer situation with $K_2 \doteq +1.1$ deg/g (as would be predicted by the simplified model if the tractor and trailer tires were reversed).

Examination of the tire data given in Appendix B shows that the tires on the tractor rear axles and the trailer tires are very much alike. Hence, it may be concluded that a small change in tire characteristics can make a large change in K_2. For example, it may be that the longitudinal slip needed to generate the drive thrust for maintaining constant forward velocity in the experiments was large enough to reduce the effective cornering stiffnesses of the tractor rear tires, thereby making the trailer understeer. But is seems more appropriate to note that K_2 is very sensitive to small errors in articulation angle or, by reversing the considerations, to state that articulation angle is primarily dependent upon the effective wheelbase, ℓ_2, and the radius of the turn, R. Specifically, for vehicles which are operated with (1) nearly equal loads on the trailer suspension and the tractor rear suspension and (2) tires with similar shear force properties, K_2 will be approximately zero and the articulation angle will be primarily a function of effective wheelbase and turn radius. Accordingly, it appears that a quick check of either simulation or test results can be obtained by comparing Γ in radians with ℓ_2/R (where Γ is the articulation angle, ℓ_2 is the distance from the center of the tractor rear suspension to the center of the trailer suspension, and R is the radius of a selected steady turn with 400 ft < R < 800 ft).

5.0 CONCLUDING REMARKS

An exceptionally good agreement between simulation and test has been achieved for obstacle-avoidance maneuvers. For severe turning maneuvers approaching wheel lift-off and rollover of the vehicle, the simulation does a reasonable job of predicting the velocity and yaw rate levels at which rollover will occur. However, vehicle performance is very sensitive to steering level, forward velocity, and vehicle parameters in severe turning maneuvers and, accordingly, very accurate input and parametric data are needed. With regard to steady turning at moderate levels of lateral acceleration, the value of trailer understeer/oversteer factor based on simulation results does not agree well with the measured value of this factor.

Based on the experience gained in this investigation, it is recommended that studies be made to develop the capability for including the influence of the steering-system properties in the simulation. Also, the influence of the drive thrust required to maintain forward velocity should be examined. Further work is needed for improving the simulation's ability to characterize the steady turning performance of both the tractor and the trailer as a function of steering-wheel angle, drive thrust, forward velocity, and yaw rate (or lateral acceleration).

The simplified analysis presented in Appendix E provides a foundation for a research program on the steady turning behavior of articulated vehicles. The various modes of static instability described in Appendix E * should be investigated. The analysis of Appendix E should be extended to include the influences of the steering system, tandem axles, roll-steer effects, and drive thrust. A program of simplified analysis, parameter measurement, vehicle testing, and simulation is recommended for obtaining a detailed understanding of the directional response properties of articulated vehicles in normal driving.

Many commercial vehicles are limited in their directional response capability due to rollover rather than saturation of tire shear force characteristics. Accordingly, for a comprehensive simulation of

---

*See pages 78, 79, and 80 for graphical illustrations of the influence of vehicle parameters on steady turning response.

directional response to be justified, the simulation should do an accurate job of predicting the roll performance of the vehicle. Although the current model appears to do reasonably well at predicting roll performance, the assumptions and approximations in the model should be reexamined with the idea of improving the prediction of roll motion. In addition, the model should be extended to permit simulation of curved, superelevated sections of roadway, thereby allowing realistic conditions for studying accident situations on existing roads.

6.0 REFERENCES

1. Motor Vehicle Manufacturers Association, "Key Issues in Heavy Truck Safety, Appendix B." Submitted at the Motor Vehicle Safety Seminar, July 12, 1976.

2. Murphy, R. W., Bernard, J.E., and Winkler, C.B. "A Computer-Based Mathematical Method for Predicting the Braking Performance of Trucks and Tractor-Trailers." Phase I Report: Motor Truck Braking and Handling Study, Highway Safety Research Institute, University of Michigan, September 15, 1972.

3. Winkler, C.B., et al. "Predicting the Braking Performance of Trucks and Tractor-Trailers." Phase III Technical Report, Report No. UM-HSRI-76-26, Highway Safety Research Institute, University of Michigan, June 1976.

4. Bernard, J.E., Winkler, C.B., and Fancher, P.S. "A Computer-Based Mathematical Method for Predicting the Directional Response of Trucks and Tractor-Trailers." Phase II Technical Report: Motor Truck Braking and Handling Performance Study, Report No. UM-HSRI-PF-73-1, Highway Safety Research Institute, University of Michigan, June 1, 1973.

5. Fancher, P.S. and MacAdam, C.C. "Computer Analysis of Antilock System Performance in the Braking of Commercial Vehicles." Paper presented at Institution of Mechanical Engineers Conference on Braking of Road Vehicles, Loughborough, England, March 1976.

6. Fancher, P.S. "Pitching and Bouncing Dynamics Excited During Antilock Braking of a Heavy Truck." Presented at 5th VSD-2nd IUTAM Symposium on Dynamics of Vehicles on Roads and Tracks, Vienna, September 19-23, 1977.

7. Gillespie, T.D. "Validation of the MVMA/HSRI Phase II Straight Truck Directional Response Simulation." Preliminary Report, Report No. UM-HSRI-78-46, Highway Safety Research Institute, University of Michigan, October 1978.

8. Moncarz, H., Bernard, J.E., Gupta, R., and Fancher, P.S. "Vehicle-In-Use Limit Performance and Tire Factors, Appendix B." Final Report, Contract No. DOT-HS-031-3-693, Report No. UM-HSRI-PF-75-1-3, Highway Safety Research Institute, University of Michigan, January 31, 1975.

9. Hill, R. "Principles of Dynamics." The MacMillan Company, New York, 1964.

10. "Truck and Trailer Yaw Divergence and Rollover." RFP-NHTSA-7-B709, Contract No. DOT-HS-7-01602, Highway Safety Research Institute, University of Michigan, to be completed April, 1979.

11. Gillespie, T.D. and Winkler, C.B. "On the Directional Response Characteristics of Heavy Vehicles." Proceedings, 5th VSD-2nd IUTAM Symposium on The Dynamics of Vehicles on Roads and Tracks, Vienna, September 19-23, 1977.

APPENDIX A

TRACTOR-VAN TRAILER PARAMETERS

Brief definitions of each parameter are given here. Additional discussions of the meaning of these parameters are given in Reference [4].

IHC-TRACTOR VAN TRLER LOADED,10X22, 10X20 FIRSTONE&FREUHAUF-TIRES-RUN#200

INPUT PARAMETER TABLE

SYMBOL	DESCRIPTION	INITIAL VALUE
KEY(1)	TRACTOR AXLE KEY: 0 FOR SINGLE AXLE 1 FOR WALKING BEAM 2 FOR 4 ELLIPTIC LEAF	2
KEY(2)	TRAILER AXLE KEY	2
AA1	HORIZONTAL DISTANCE FORM TRACTOR FRONT LEAF-FRAME CONTACT TO AXLE CENTER (IN)	24.00
AA2	HORIZONTAL DISTANCE FROM TRACTOR REAR LEAF-FRAME CONTACT TO AXLE CENTER (IN)	24.00
AA4	HORIZONTAL DISTANCE FROM TRACTOR FRONT LEAF-FRAME CONTACT TO LOAD LEVELER PIN (IN	1.00
AA5	HORIZONTAL DISTANCE FROM TRACTOR REAR LEAF-FRAME CONTACT TO LOAD LEVELER PIN (IN	1.00
AA6	VERTICAL DISTANCE FROM AXLE DOWN TO TRACTOR TORQUE ROD (IN)	0.0
AA7	ANGLE BETWEEN TRACTOR TORQUE ROD AND HORIZONTAL (DEG)	0.0
AA8	HORIZONTAL DISTANCE FROM AXLE CENTER FORWARD TO TRACTOR TORQUE ROD (IN)	0.0
AA9	HORIZONTAL DISTANCE FROM TRAILER FRONT LEAF-FRAME CONTACT TO AXLE CENTER (IN)	18.50
AA10	HORIZONTAL DISTANCE FROM TRAILER REAR LEAF-FRAME CONTACT TO AXLE CENTER (IN)	18.50
AA12	HORIZONTAL DISTANCE FROM TRAILER FRONT LEAF-FRAME CONTACT TO LOAD LEVELER PIN (IN	6.25
AA13	HORIZONTAL DISTANCE FROM TRAILER REAR LEAF-FRAME CONTACT TO LOAD LEVELER PIN (IN	6.25
AA14	VERTICAL DISTANCE FROM AXLE DOWN TO TRAILER TORQUE ROD (IN)	7 00
AA15	ANGLE BETWEEN TRAILER TORQUE ROD AND HORIZONTAL (DEG)	15.01
AA16	HORIZONTAL DISTANCE FROM AXLE CENTER FORWARD TO TRAILER TORQUE ROD (IN)	5.50
A1	HORIZONTAL DISTANCE FROM TRACTOR CG TO CENTER OF TRACTOR FRONT SUSPENSION (IN)	35.90
A2	HORIZONTAL DISTANCE FROM TRACTOR CG TO CENTER OF TRACTOR REAR SUSPENSION (IN)	106.10
A3	HORIZONTAL DISTANCE FROM TRAILER CG TO 5TH WHEEL (IN)	230.50
A4	HORIZONTAL DISTANCE FROM TRAILER CG TO CENTER OF TRAILER SUSPENSION (IN)	179.50
ALPHA1	STATIC DISTANCE, TRACTOR FRONT AXLE TO GROUND (IN)	20.30
ALPHA2	STATIC DISTANCE, TRACTOR REAR AXLE(S) TO GROUND (IN)	20.30
ALPHA3	STATIC DISTANCE, TRAILER AXLE(S) TO GROUND (IN)	19.50
AN1	TIRE PRESSURE DIST. FUNCTION FOR TRACTOR FRONT TIRES	0.250
AN2	TIRE PRESSURE DIST. FUNCTION FOR TRACTOR FRONT TANDEM TIRES	0.250
AN3	TIRE PRESSURE DIST. FUNCTION FOR TRACTOR REAR TANDEM TIRES	0.250
AN4	TIRE PRESSURE DIST. FUNCTION FOR TRAILOR FRONT TANDEM TIRES	0.250
AN5	TIRE PRESSURE DIST. FUNCTION FOR TRAILOR REAR TANDEM TIRES	0.250
BB	HORIZONTAL DISTANCE FROM 5TH WHEEL TO MIDPOINT OF TRACTOR REAR SUSPENSION (IN)	0.0
C1	VISCOUS DAMPING: JOUNCE ON TRACTOR FRONT SUSPENSION (LB-SEC/IN)	10.00
C2	VISCOUS DAMPING: REBOUND ON TRACTOR FRONT SUSPENSION (LB-SEC/IN)	20.00
C3	VISCOUS DAMPING: JOUNCE ON TRACTOR REAR SUSPENSION (LB-SEC/IN)	10.00
C4	VISCOUS DAMPING: REBOUND ON TRACTOR REAR SUSPENSION (LB-SEC/IN)	20.00
C5	VISCOUS DAMPING: JOUNCE ON TRAILER SUSPENSION (LB-SEC/IN)	0.0
C6	VISCOUS DAMPING: REBOUND ON TRAILER SUSPENSION (LB-SEC/IN)	0.0

CALF1	LATERAL STIFFNESS, TRACTOR FRONT TIRES (LBS/DEG)	-1.00
CF1	MAXIMUM COULOMB FRICTION, TRACTOR FRONT SUSPENSION (LB)	500.00
CF2	MAXIMUM COULOMB FRICTION, TRACTOR REAR SUSPENSION (LB)	500.00
CF3	MAXIMUM COULOMB FRICTION, TRAILER SUSPENSION (LB)	3000.00
CS1	LONGITUDINAL STIFFNESS, TRACTOR FRONT TIRES (LBS)	-1.00
CS2	LONGITUDINAL STIFFNESS, TRACTOR FRONT TANDEM TIRES (LBS)	-1.00
CS3	LONGITUDINAL STIFFNESS, TRACTOR REAR TANDEM TIRES (LBS)	-1.00
CS4	LONGITUDINAL STIFFNESS, TRAILER FRONT TANDEM TIRES (LBS)	-1.00
CS5	LONGITUDINAL STIFFNESS, TRAILER REAR TANDEM TIRES (LBS)	-1.00
D	VERTICAL DISTANCE FROM 5TH WHEEL CONNECTION TO TRACTOR CG (IN)	8.80
DELTA1	STATIC VERTICAL DISTANCE, TRACTOR CG TO TRACTOR FRONT AXLE (IN)	19.40
DELTA3	STATIC VERTICAL DISTANCE, TRAILER CG TO TRAILER AXLE (IN)	37.80
DT2	DISTANCE BETWEEN DUAL TIRES, TRACTOR REAR SUSPENSION (IN)	13.00
DT3	DISTANCE BETWEEN DUAL TIRES, TRAILER SUSPENSION (IN)	13.00
FA1	FRICTION REDUCTION PARAMETER FOR TRACTOR FRONT TIRES	0.0
FA2	FRICTION REDUCTION PARAMETER FOR TRACTOR FRONT TANDEM TIRES	0.0
FA3	FRICTION REDUCTION PARAMETER FOR TRACTOR REAR TANDEM TIRES	0.0
FA4	FRICTION REDUCTION PARAMETER FOR TRAILER FRONT TANDEM TIRES	0.0
FA5	FRICTION REDUCTION PARAMETER FOR TRAILER REAR TANDEM TIRES	0.0
IXX	TRACTOR SPRUNG MASS ROLL MOMENT OF INERTIA (IN-LB-SEC**2)	18166.00
IYY	TRACTOR SPRUNG MASS PITCH MOMENT OF INERTIA (IN-LB-SEC**2)	69955.00
IZZ	TRACTOR YAW MOMENT OF INERTIA (IN-LB-SEC**2)	69955.00
IXZ	TRACTOR PITCH PLANE CROSS MOMENT (IN-LB-SEC**2)	0.0
ITXX	TRAILER SPRUNG MASS ROLL MOMENT OF INERTIA (IN-LB-SEC**2)	73000.00
ITYY	(IN-LB-SEC**2) MASS PITCH MOMENT OF INER	789869.00
ITZZ	TRAILER YAW MOMENT OF INERTIA (IN-LB-SEC**2)	789869.00
ITXZ	TRAILER PITCH PLANE CROSS MOMENT (IN-LB-SEC**2)	0.0
JA1	ROLL MOMENT OF TRACTOR FRONT AXLE (IN-LB-SEC**2)	3719.00
JA2	ROLL MOMENT OF TRACTOR FRONT TANDEM AXLE (IN-LB-SEC**2)	4458.00
JA3	ROLL MOMENT OF TRAILER FRONT TANDEM AXLE (IN-LB-SEC**2)	4100.00
JS1	POLAR MOMENT OF TRACTOR FRONT WHEELS (IN-LB-SEC**2)	103.00
JS2	POLAR MOMENT OF TRACTOR FRONT TANDEM WHEELS (IN-LB-SEC**2)	231.00
JS3	POLAR MOMENT OF TRACTOR REAR TANDEM WHEELS (IN-LB-SEC**2)	231.00
JS4	POLAR MOMENT OF TRAILER FRONT TANDEM WHEELS (IN-LB-SEC**2)	231.00
JS5	POLAR MOMENT OF TRAILER REAR TANDEM WHEELS (IN-LB-SEC**2)	231.00
K1	SPRING RATE, TRACTOR FRONT SUSPENSION (LB/IN)	1012.50
K2	SPRING RATE, TRACTOR REAR SUSPENSION (LB/IN)	3000.00
K3	SPRING RATE, TRAILER SUSPENSION (LB/IN)	19175.00

KRS1	FRONT AUXILIARY ROLL STIFFNESS(IN-LB/DEG	4000.00
KRS2	REAR AUXILIARY ROLL STIFFNESS(IN-LB/DEG	0.0
KRS3	TRAILER AUXILIARY ROLL STIFFNESS(IN-LB/DEG	0.0
AKRS	TRACTOR TR TANDEM AUX ROLL STIFFNESS(IN-LB/DEG)	78000.00
KT1	SPRING RATE, TRACTOR FRONT TIRES (LB/IN)	5700.00
KT2	SPRING RATE, TRACTOR FRONT TANDEM TIRES (LB/IN)	5700.00
KT3	SPRING RATE, TRACTOR REAR TANDEM TIRES (LB/IN)	5700.00
KT4	SPRING RATE, TRAILER FRONT TANDEM TIRES (LB/IN)	5300.00
KT5	SPRING RATE, TRAILER REAR TANDEM TIRES (LB/IN)	5300.00

FIFTH WHEEL SPRING RATE

ROTATION WH5DFL (DEG)	SPRING RATE MC5 (IN-LBS/DEG)
0.0	0.20000E+08

TRACTOR FRAME ROLL SPRING RATE

ROTATION TTDFL(DEG)	SPRING RATE TTC(IN-LBS/DEG)
0.0	0.20000E+05

TRSTF	TRAILER FRAME ROLL STIFFNESS(IN-LB/DEG)	1500000.00
PW	WEIGHT OF PAYLOAD (LBS)	40600.00
PJ1	POLL MOMENT OF INERTIA OF PAYLOAD (IN-LB-SEC**2)	37500.00
PJ2	PITCH MOMENT OF INERTIA OF PAYLOAD (IN-LB-SEC**2)	1727000.00
PJ3	YAW MOMENT OF INERTIA OF PAYLOAD (IN-LB-SEC**2)	1727000.00
PX	HORIZONTAL DISTANCE FROM MIDPOINT OF REAR SUSPENSION TO PAYLOAD MASS CENTER (IN)	182.00
PZ	VERTICAL DISTANCE FROM GROUND TO PAYLOAD MASS CENTER (IN)	64.50
RCH1	ROLL CENTER HEIGHT, TRACTOR FRONT SUSPENSION (IN)	24.55
RCH2	ROLL CENTER HEIGHT, TRACTOR REAR SUSPENSION (IN)	22.00
RCH3	ROLL CENTER HEIGHT, TRAILER SUSPENSION (IN	25.60
RS1	COMPLIANCE STEER (DEG/IN)	0.0
RSC1	ROLL STEER COEFFICIENT, TRACTOR FRONT SUSPENSION	0.0
RSC2	ROLL STEER COEFFICIENT, TRACTOR REAR SUSPENSION	0.10
RSC3	ROLL STEER COEFFICIENT, TRAILER SUSPENSION	0.10
SY1	HORIZONTAL DISTANCE FROM TRACTOR BODY X-AXIS TO TRACTOR FRONT SUSPENSION (IN)	16.30
SY2	HORIZONTAL DISTANCE FROM TRACTOR BODY X-AXIS TO TRACTOR REAR SUSPENSION (IN)	17.50
SY3	HORIZONTAL DISTANCE FROM TRAILER BODY X-AXIS TO TRAILER SUSPENSION (IN)	19.00
TIMF	MAXIMUM REAL TIME FOR SIMULATION (SEC)	0.10
TRA1	HALF TRACK, TRACTOR FRONT AXLE (IN)	40.25
TRA2	HALF TRACK, TRACTOR REAR AXLE(S) (IN)	36.00
TRA3	HALF TRACK, TRAILER AXLE(S) (IN)	36.00
VEL	INITIAL VELOCITY (FT/SEC)	66.00
W1	SPRUNG WEIGHT OF TRACTOR (LBS)	10316.00
W2	SPRUNG WEIGHT OF TRAILER (LBS)	14281.00
WS1	WEIGHT OF TRACTOR FRONT SUSPENSION (LBS)	1190.00
WS2	WEIGHT OF TRACTOR FRONT TANDEM SUSPENSION (LBS)	2340.00
WS3	WEIGHT OF TRACTOR REAR TANDEM SUSPENSION (LBS)	2170.00
WS4	WEIGHT OF TRAILER FRONT TANDEM SUSPENSION (LBS)	1520.00
WS5	WEIGHT OF TRAILER REAR TANDEM SUSPENSION (LBS)	1520.00

```
BRAKE PARAMETERS: TQ(1,1,1) = 0.050 TQ(1,1,2) = 0.270
                  TQ(1,2,1) = 0.050 TQ(1,2,2) = 0.270
                  TQ(2,1,1) = 0.075 TQ(2,1,2) = 0.245
                  TQ(2,2,1) = 0.075 TQ(2,2,2) = 0.245
                  TQ(3,1,1) = 0.075 TQ(3,1,2) = 0.245
                  TQ(3,2,1) = 0.075 TQ(3,2,2) = 0.245
                  TQ(4,1,1) = 0.175 TQ(4,1,2) = 0.303
                  TQ(4,2,1) = 0.175 TQ(4,2,2) = 0.303
                  TQ(5,1,1) = 0.175 TQ(5,1,2) = 0.303
                  TQ(5,2,1) = 0.175 TQ(5,2,2) = 0.303

    TABLE 1: TIME VS PRESSURE (PSI)
             NO. OF POINTS:  2
          0.0           0.0
          0.0500        0.0

    INPUT PARAMETER TABLE FOR BRAKE FORCE CALCULATION SUBROUTINE
    SYMBOL      DESCRIPTION                              INITIAL VALUE
                                AXLE 1, LEFT SIDE
    IBRT        BRAKE TYPE                                      NONE
                                AXLE 2, LEFT SIDE
    IBRT        BRAKE TYPE                                      NONE
                                AXLE 3, LEFT SIDE
    IBRT        BRAKE TYPE                                      NONE
                                AXLE 4, LEFT SIDE
    IBRT        BRAKE TYPE                                      NONE
                                AXLE 5, LEFT SIDE
    IBRT        BRAKE TYPE                                      NONE

    ALIGNING TORQUE LOOK-UP, TRACTOR FRONT TIRES
        VERTICAL LOAD:   2000.000 LBS
            SIDESLIP ANGLE (DEG) VS ALIGNING TORQUE (IN-LBS)
             0.0           0.0
             1.000        44.000
             3.000        77.000
             7.000        79.000
            10.000        59.000
        VERTICAL LOAD:   4000.000 LBS
            SIDESLIP ANGLE (DEG) VS ALIGNING TORQUE (IN-LBS)
             0.0           0.0
             1.000       103.000
             3.000       205.000
             7.000       245.000
            10.000       189.000
        VERTICAL LOAD:   6000.000 LBS
            SIDESLIP ANGLE (DEG) VS ALIGNING TORQUE (IN-LBS)
             0.0           0.0
             1.000       153.000
             3.000       341.000
             7.000       435.000
            10.000       333.000
        VERTICAL LOAD:   8000.000 LBS
            SIDESLIP ANGLE (DEG) VS ALIGNING TORQUE (IN-LBS)
             0.0           0.0
             1.000       205.000
             3.000       472.000
             7.000       600.000
            10.000       470.000
        VERTICAL LOAD:   9000.000 LBS
            SIDESLIP ANGLE (DEG) VS ALIGNING TORQUE (IN-LBS)
             0.0           0.0
             1.000       227.000
             3.000       537.000
             7.000       673.000
            10.000       550.000
```

```
ALIGNING TORQUE LOOK-UP, TRACTOR LEADING TANDEM TIRES
    VERTICAL LOAD:   2000.000 LBS
        SIDESLIP ANGLE (DEG) VS ALIGNING TORQUE (IN-LBS)
         0.0           0.0
         1.000        44.000
         3.000        77.000
         7.000        79.000
        10.000        59.000
    VERTICAL LOAD:   4000.000 LBS
        SIDESLIP ANGLE (DEG) VS ALIGNING TORQUE (IN-LBS)
         0.0           0.0
         1.000       103.000
         3.000       205.000
         7.000       245.000
        10.000       189.000
    VERTICAL LOAD:   6000.000 LBS
        SIDESLIP ANGLE (DEG) VS ALIGNING TORQUE (IN-LBS)
         0.0           0.0
         1.000       153.000
         3.000       341.000
         7.000       435.000
        10.000       333.000
    VERTICAL LOAD:   8000.000 LBS
        SIDESLIP ANGLE (DEG) VS ALIGNING TORQUE (IN-LBS)
         0.0           0.0
         1.000       205.000
         3.000       472.000
         7.000       600.000
        10.000       470.000
    VERTICAL LOAD:   9000.000 LBS
        SIDESLIP ANGLE (DEG) VS ALIGNING TORQUE (IN-LBS)
         0.0           0.0
         1.000       227.000
         3.000       537.000
         7.000       673.000
        10.000       550.000

ALIGNING TORQUE LOOK-UP, TRACTOR TRAILING TANDEM TIRES
    VERTICAL LOAD:   2000.000 LBS
        SIDESLIP ANGLE (DEG) VS ALIGNING TORQUE (IN-LBS)
         0.0           0.0
         1.000        44.000
         3.000        77.000
         7.000        79.000
        10.000        59.000
    VERTICAL LOAD:   4000.000 LBS
        SIDESLIP ANGLE (DEG) VS ALIGNING TORQUE (IN-LBS)
         0.0           0.0
         1.000       103.000
         3.000       205.000
         7.000       245.000
        10.000       189.000
    VERTICAL LOAD:   6000.000 LBS
        SIDESLIP ANGLE (DEG) VS ALIGNING TORQUE (IN-LBS)
         0.0           0.0
         1.000       153.000
         3.000       341.000
         7.000       435.000
        10.000       333.000
    VERTICAL LOAD:   8000.000 LBS
        SIDESLIP ANGLE (DEG) VS ALIGNING TORQUE (IN-LBS)
         0.0           0.0
         1.000       205.000
         3.000       472.000
         7.000       600.000
        10.000       470.000
    VERTICAL LOAD:   9000.000 LBS
        SIDESLIP ANGLE (DEG) VS ALIGNING TORQUE (IN-LBS)
         0.0           0.0
         1.000       227.000
         3.000       537.000
         7.000       673.000
        10.000       550.000
```

```
ALIGNING TORQUE LOOK-UP, TRAILER LEADING TANDEM TIRES
    VERTICAL LOAD:   2000.000 LBS
        SIDESLIP ANGLE (DEG) VS ALIGNING TORQUE (IN-LBS)
         0.0           0.0
         1.000        39.000
         3.000        75.000
         7.000        77.000
        10.000        49.000
    VERTICAL LOAD:   4000.000 LBS
        SIDESLIP ANGLE (DEG) VS ALIGNING TORQUE (IN-LBS)
         0.0           0.0
         1.000        96.000
         3.000       204.000
         7.000       250.000
        10.000       192.000
    VERTICAL LOAD:   6000.000 LBS
        SIDESLIP ANGLE (DEG) VS ALIGNING TORQUE (IN-LBS)
         0.0           0.0
         1.000       147.000
         3.000       343.000
         7.000       457.000
        10.000       383.000
    VERTICAL LOAD:   8000.000 LBS
        SIDESLIP ANGLE (DEG) VS ALIGNING TORQUE (IN-LBS)
         0.0           0.0
         1.000       194.000
         3.000       481.000
         7.000       650.000
        10.000       535.000
    VERTICAL LOAD:   9000.000 LBS
        SIDESLIP ANGLE (DEG) VS ALIGNING TORQUE (IN-LBS)
         0.0           0.0
         1.000       217.000
         3.000       555.000
         7.000       766.000
        10.000       671.000

ALIGNING TORQUE LOOK-UP, TRAILER TRAILING TANDEM TIRES
    VERTICAL LOAD:   2000.000 LBS
        SIDESLIP ANGLE (DEG) VS ALIGNING TORQUE (IN-LBS)
         0.0           0.0
         1.000        39.000
         3.000        75.000
         7.000        77.000
        10.000        49.000
    VERTICAL LOAD:   4000.000 LBS
        SIDESLIP ANGLE (DEG) VS ALIGNING TORQUE (IN-LBS)
         0.0           0.0
         1.000        96.000
         3.000       204.000
         7.000       250.000
        10.000       192.000
    VERTICAL LOAD:   6000.000 LBS
        SIDESLIP ANGLE (DEG) VS ALIGNING TORQUE (IN-LBS)
         0.0           0.0
         1.000       147.000
         3.000       343.000
         7.000       457.000
        10.000       383.000
    VERTICAL LOAD:   8000.000 LBS
        SIDESLIP ANGLE (DEG) VS ALIGNING TORQUE (IN-LBS)
         0.0           0.0
         1.000       194.000
         3.000       481.000
         7.000       650.000
        10.000       535.000
    VERTICAL LOAD:   9000.000 LBS
        SIDESLIP ANGLE (DEG) VS ALIGNING TORQUE (IN-LBS)
         0.0           0.0
         1.000       217.000
         3.000       555.000
         7.000       766.000
        10.000       671.000
```

TABLE 2: TIME VS STEER ANGLE (DEG)
LEFT SIDE
NO. OF POINTS: 4

0.0	0.0
0.6000	-2.6500
4.0000	-2.6500
6.0000	-2.6500

TABLE 3: TIME VS STEER ANGLE (DEG)
RIGHT SIDE
NO. OF POINTS: 4

0.0	0.0
0.6000	-2.4000
4.0000	-2.4000
6.0000	-2.4000

TABLE 4: VERTICAL LOAD VS LATERAL STIFFNESS (LBS/DEG)
TRACTOR FRONT TIRES
NO. OF POINTS 6

0.0	0.0	1.0000	10.0000
2000.0000	465.0000	1.0000	10.0000
4000.0000	690.0000	1.0000	10.0000
6000.0000	820.0000	1.0000	10.0000
8000.0000	880.0000	1.0000	10.0000
9000.0000	880.0000	1.0000	10.0000

TABLE 5: VERTICAL LOAD VS LATERAL STIFFNESS (LBS/DEG)
TRACTOR LEADING TANDEM TIRES
NO. OF POINTS 6

0.0	0.0	1.0000	10.0000
2000.0000	465.0000	1.0000	10.0000
4000.0000	690.0000	1.0000	10.0000
6000.0000	820.0000	1.0000	10.0000
8000.0000	880.0000	1.0000	10.0000
9000.0000	880.0000	1.0000	10.0000

TABLE 6: VERTICAL LOAD VS LATERAL STIFFNESS (LBS/DEG)
TRACTOR TRAILING TANDEM TIRES
NO. OF POINTS 6

0.0	0.0	1.0000	10.0000
2000.0000	465.0000	1.0000	10.0000
4000.0000	690.0000	1.0000	10.0000
6000.0000	820.0000	1.0000	10.0000
8000.0000	880.0000	1.0000	10.0000
9000.0000	880.0000	1.0000	10.0000

TABLE 7: VERTICAL LOAD VS LATERAL STIFFNESS (LBS/DEG)
TRAILER LEADING TANDEM TIRES
NO. OF POINTS 6

0.0	0.0	0.5000	10.0000
2000.0000	400.0000	0.5000	10.0000
4000.0000	600.0000	0.5000	10.0000
6000.0000	720.0000	0.5000	10.0000
8000.0000	770.0000	0.5000	10.0000
9000.0000	770.0000	0.5000	10.0000

TABLE 8: VERTICAL LOAD VS LATERAL STIFFNESS (LBS/DEG)
TRAILER TRAILING TANDEM TIRES
NO. OF POINTS 6

0.0	0.0	0.5000	10.0000
2000.0000	400.0000	0.5000	10.0000
4000.0000	600.0000	0.5000	10.0000
6000.0000	720.0000	0.5000	10.0000
8000.0000	770.0000	0.5000	10.0000
9000.0000	770.0000	0.5000	10.0000

TABLE 9: VERTICAL LOAD VS LONGITUDINAL STIFFNESS (LBS)
TRACTOR FRONT TIRES
NO. OF POINTS: 1

0.0	28000.0000

TABLE 10: VERTICAL LOAD VS LONGITUDINAL STIFFNESS (LBS)
TRACTOR LEADING TANDEM TIRES
NO. OF POINTS: 1

0.0	28000.0000

TABLE 11: VERTICAL LOAD VS LONGITUDINAL STIFFNESS (LBS)
TRACTOR TRAILING TANDEM TIRES
NO. OF POINTS: 1

0.0	28000.0000

TABLE 12: VERTICAL LOAD VS LONGITUDINAL STIFFNESS (LBS)
TRAILER LEADING TANDEM TIRES
NO. OF POINTS: 1

0.0	28000.0000

TABLE 13: VERTICAL LOAD VS LONGITUDINAL STIFFNESS (LBS)
TRAILER TRAILING TANDEM TIRES
NO. OF POINTS: 1

0.0	28000.0000

TABLE 14: VERTICAL LOAD VS MUZERO
TRACTOR FRONT TIRES
NO. OF POINTS: 6

0.0	1.0700
2000.0000	1.0700
4000.0000	0.9800
6000.0000	0.8800
8000.0000	0.8300
9000.0000	0.8300

TABLE 15: VERTICAL LOAD VS MUZERO
TRACTOR LEADING TANDEM TIRES
NO. OF POINTS: 6

0.0	1.0700
2000.0000	1.0700
4000.0000	0.9800
6000.0000	0.8800
8000.0000	0.8300
9000.0000	0.8300

TABLE 16: VERTICAL LOAD VS MUZERO
TRACTOR TRAILING TANDEM TIRES
NO. OF POINTS: 6

0.0	1.0700
2000.0000	1.0700
4000.0000	0.9800
6000.0000	0.8800
8000.0000	0.8300
9000.0000	0.8300

TABLE 17: VERTICAL LOAD VS MUZERO
TRAILER LEADING TANDEM TIRES
NO. OF POINTS: 6

0.0	1.0400
2000.0000	1.0400
4000.0000	0.9800
6000.0000	0.9200
8000.0000	0.8800
9000.0000	0.8800

```
    TABLE 18:  VERTICAL LOAD VS MUZERO
               TRAILER TRAILING TANDEM TIRES
               NO. OF POINTS:  6
          0.0            1.0400
       2000.0000         1.0400
       4000.0000         0.9800
       6000.0000         0.9200
       8000.0000         0.8800
       9000.0000         0.8800

    PARAMETERS FOR INCLINE SURFACE:
          G1          GRAVITY X COMPONENT          0.0
          G2          GRAVITY Y COMPONENT          0.0
          G3          GRAVITY Z COMPONENT          1.000

    THERE WILL BE NO WIND THIS RUN

THE ANTILOCK SYSTEM WILL NOT BE USED THIS RUN

     *** END INPUT ***
```

	EMPTY	LOADED
DISTANCE FROM TRAILER SPRUNG MASS CENTER TO TRAILER REAR AXLE CENTERLINE (IN)	179.500	181.349
DISTANCE FROM TRAILER SPRUNG MASS CENTER TO GROUND (IN)	57.300	62.626
ROLL MOMENT OF TRAILER SPRUNG MASS (IN-LB-SEC**2)	72999.938	111918.563
PITCH MOMENT OF TRAILER SPRUNG MASS (IN-LB-SEC**2)	789868.500	2518456.000
YAW MOMENT OF TRAILER SPRUNG MASS (IN-LB-SEC**2)	789868.500	2517038.000

THE STATIC LOADS ON THE TIRES ARE

AXLE NUMBER	LOAD
1	8897.938
2	15781.398
3	15611.398
4	16823.133
5	16823.133
TOTAL	73937.000

```
THE TRACTOR TOTAL SPRUNG MASS CENTER IS       62.844 INCHES BEHIND THE FRONT AXLE,
THE TOTAL YAW MOMENT OF INERTIA IS   192914.500 IN LB SEC**2.

THE TRAILER MASS CENTER IS      238.169 INCHES BEHIND THE FIFTH WHEEL,
THE TOTAL YAW MOMENT OF INERTIA IS  2775432.000 IN LB SEC**2

TIME INCREMENT TO BE PRINTED OUT IS 0.10

 *** BEGIN OUTPUT ***
```

APPENDIX B

TIRE DATA

FIRESTONE 10.00 x 22 F

F_y (LATERAL FORCE)

F_z (lb)	1°	3°	4°	5°	7°	10°
2000	436	1065	1311	1506	1794	2044
4000	635	1657	2072	2430	2957	3442
6000	764	2021	2539	3019	3704	4422
8000	831	2225	2827	3384	4190	5086
9000	830	2284	2909	3487	4341	5319

M_z (ALIGNING TORQUE)

F_z (lb)	1°	3°	4°	5°	7°	10°
2000	44	77	84	85	79	59
4000	103	205	236	252	245	189
6000	153	341	396	431	435	333
8000	205	472	558	622	600	470
9000	227	537	637	716	673	550

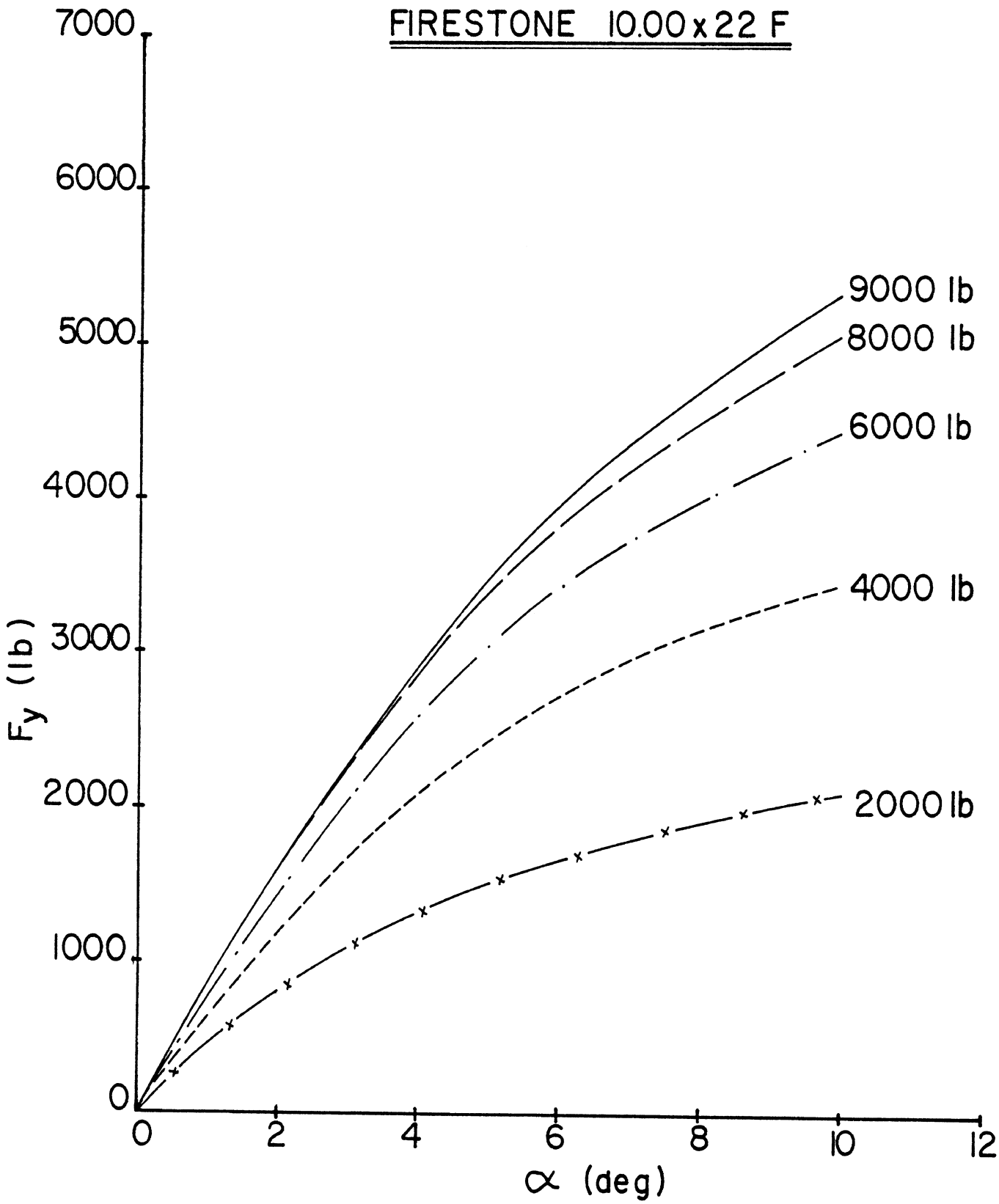
FIRESTONE 10.00x22 F
7000
6000
5000
4000
3000
2000
1000
0
Fy (lb)
9000 lb
8000 lb
6000 lb
4000 lb
2000 lb
0
2
4
6
8
10
12
α (deg)

FIRESTONE 10.00x20 RIB

F_y (LATERAL FORCE)

F_z (lb)	1°	3°	4°	5°	7°	10°
2000	356	824	1018	1221	1502	1767
4000	580	1421	1770	2123	2612	3171
6000	701	1808	2259	2711	3378	4182
8000	767	2032	2583	3072	3849	4861
9000	784	2104	2674	3182	4020	5056

M_z (ALIGNING TORQUE)

F_z (lb)	1°	3°	4°	5°	7°	10°
2000	31	44	46	56	61	39
4000	80	143	157	189	194	158
6000	130	261	299	354	373	329
8000	179	387	459	532	562	473
9000	200	452	533	624	650	565

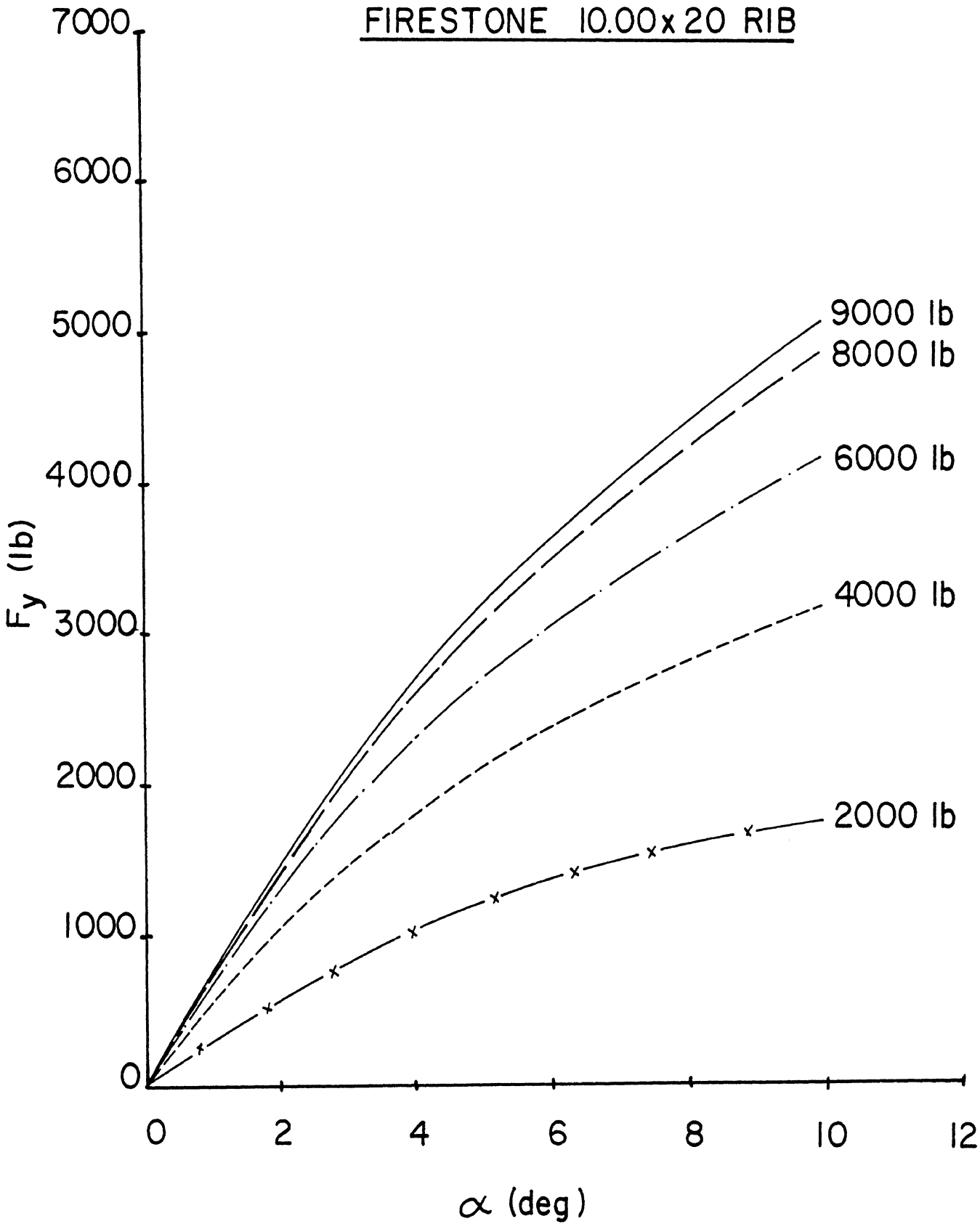
FIRESTONE 10.00x20 RIB
7000
6000
5000
4000
3000
2000
1000
0
F_y (lb)
9000 lb
8000 lb
6000 lb
4000 lb
2000 lb
0
2
4
6
8
10
12
α (deg)

FREUHAUF 10.00 x 20

F_y (LATERAL FORCE)

F_z (lb)	1°	3°	4°	5°	7°	10°
2000	365	936	1171	1371	1660	1935
4000	556	1503	1910	2283	2814	3400
6000	686	1858	2363	2821	3570	4408
8000	739	2025	2596	3135	4012	5030
9000	742	2058	2646	3213	4131	5256

M_z (ALIGNING TORQUE)

F_z (lb)	1°	3°	4°	5°	7°	10°
2000	39	75	81	86	77	49
4000	96	204	238	259	250	192
6000	147	343	407	448	457	383
8000	194	481	579	646	650	535
9000	217	555	664	736	766	671

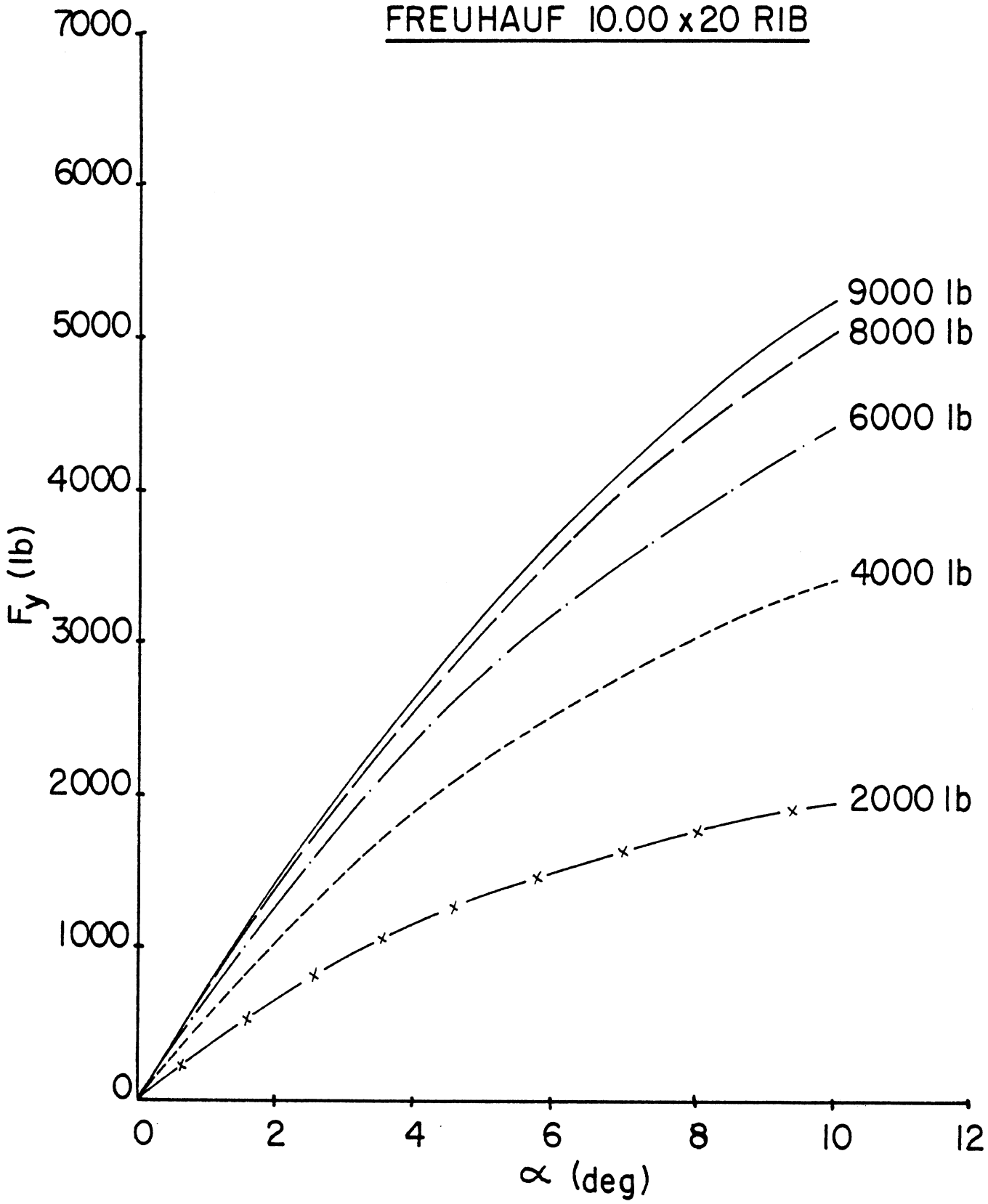
FREUHAUF 10.00 x 20 RIB
7000
6000
5000
4000
3000
2000
1000
0
F_y (lb)
9000 lb
8000 lb
6000 lb
4000 lb
2000 lb
0
2
4
6
8
10
12
∝ (deg)

APPENDIX C

The purpose of this appendix is to provide a condensed description of the simulation model used in this study. Although the model is intended for studying both braking and turning, this discussion emphasizes features of the model which are pertinent to investigating the directional response to steering.

C.1 Axis Systems

For each unit of the vehicle (tractor or semitrailer), three axis systems are employed. These systems are (1) a set of inertial reference axes, (2) a set of body axes for the sprung mass, and (3) an auxiliary set of axes lying in the road plane below the center of mass of the sprung mass. The simulation is arranged so that the inertial system has its origin at the sprung mass center of gravity at time zero.

For descriptive purposes, it is convenient to use sets of unit vectors to represent the three "right-handed" orthogonal axis systems used in the model, viz.:

$[\hat{x}_n\ \hat{y}_n\ \hat{z}_n]$ represent the inertial system

$[\hat{x}_b\ \hat{y}_b\ \hat{z}_b]$ represent the body axis system

$[\hat{x}_l\ \hat{y}_l\ \hat{z}_l]$ represent the road axis system

These axis systems are illustrated in Figure C.1.

The relationships allowed between these axis systems are constrained in the computer model. The "road" is assumed to be a flat surface extending indefinitely in space. The $\hat{x}_l$ and $\hat{y}_l$ unit vectors lie in the road plane. (The road can be inclined with respect to gravity.) The plane defined by the $\hat{x}_n$ and $\hat{y}_n$ unit vectors is parallel to the road plane. The $\hat{z}_n$ and $\hat{z}_l$ unit vectors are colinear and the $\hat{x}_l\hat{y}_l\hat{z}_l$ system can rotate in heading angle, ψ, with respect to the

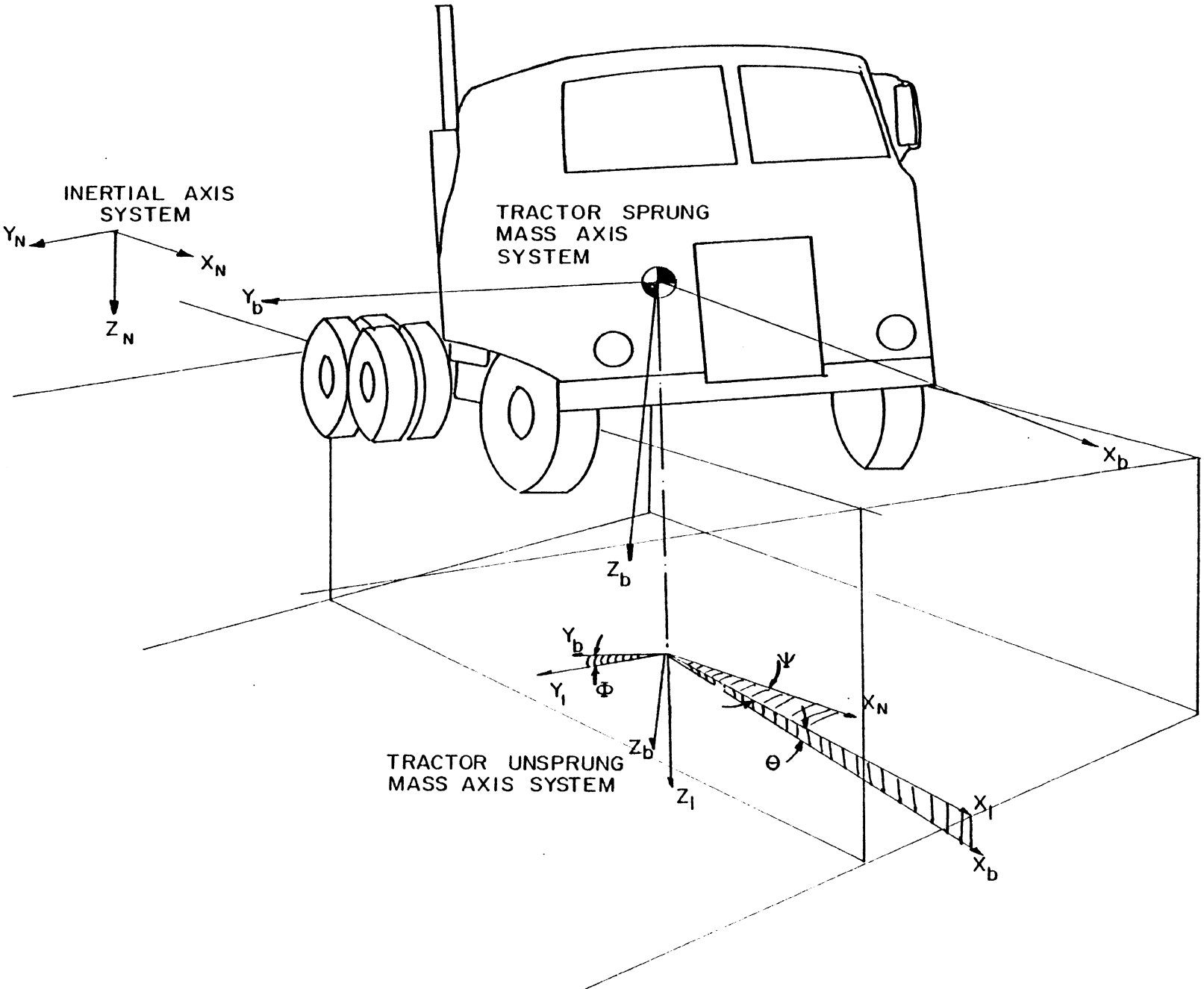

Figure C.1. Axis systems

$\hat{x}_n\hat{y}_n\hat{z}_n$ system. The center of the $\hat{x}_l\hat{y}_l\hat{z}_l$ axis system is taken to be "directly below" (that is, in the direction of the $\hat{z}_n$ and $\hat{z}_l$ unit vectors) the center of the body axis system. The orientation of the $\hat{x}_b\hat{y}_b\hat{z}_b$ unit vectors with respect to the $\hat{x}_l\hat{y}_l\hat{z}_l$ unit vectors is described by two rotations in the following order. First, a pitch, θ, about the $\hat{y}_l$ axis and then a roll, ϕ, about the $\hat{x}_b$ axis.

The angles ψ, θ, and ϕ are a set of Euler angles" defining the orientation of the sprung-mass body axes with respect to the inertial axes. Standard sets of differential equations for the time rates of change of the Euler angles are solved in the computer model to obtain instantaneous values of ψ, θ, and ϕ. Knowing ψ, θ, and ϕ, vectors expressed in one axis system can be transformed into either of the other two axis systems.*

C.2 Sprung Mass Motion

The motion of the sprung mass is simulated using standard equations describing the motion of a rigid body in a rotating coodinate system [9], viz.,

$$m\dot{\overline{V}} = \overline{F} \qquad (C.1)$$

and

$$\dot{\overline{H}} = \overline{T} \qquad (C.2)$$

where m is the sprung mass

$\dot{\overline{V}}$ is the acceleration of the center of gravity of the sprung mass

$\overline{F}$ is the total force applied to the sprung mass

$\dot{\overline{H}}$ is the time rate of change of the moment of momentum

and $\overline{T}$ is the total torque applied to the sprung mass

Discussion of the components of $\overline{F}$ and $\overline{T}$ will be presented in a later section of this appendix.

---

*In order to condense the presentation, a working knowledge of Euler angles, vector-matrix equations, moving coordinate systems, and rigid body dynamics is assumed.

Defining the velocity $\bar{V}$ as $u\,\hat{x}_b + v\,\hat{y}_b + w\,\hat{z}_b$ and the spin velocity, $\bar{\omega}$, as $p\,\hat{x}_b + q\,\hat{y}_b + r\,\hat{z}_b$, and carrying out the necessary differentiations yields:

$$\dot{\bar{V}} = (\dot{u} + qw - rv)\hat{x}_b + (\dot{v} - pw + ru)\hat{y}_b + (\dot{w} + pv - qu)\hat{z}_b \quad (C.3)$$

Also, it can be shown that

$$\dot{\bar{H}} = [I_{xx}\dot{p} + qr(I_{zz}-I_{yy}) - I_{xz}(\dot{r} + pq)]\hat{x}_b + [I_{yy}\dot{q} + pr(I_{xx}-I_{zz}) - I_{xz}(r^2-p^2)]\hat{y}_b + [I_{zz}\dot{r} + pq(I_{yy}-I_{xx}) + I_{xz}(qr-\dot{p})]\hat{z}_b \quad (C.4)$$

where (for the sprung mass)

I_{xx} is the roll moment of inertia

I_{yy} is the pitch moment of inertia

I_{zz} is the yaw moment of inertia

$$I_{xz} = \int_{\text{mass}} xz\ dm$$

(Lateral symmetry is assumed so that $I_{xy} = I_{yz} = 0.$)

Based on Equations (C.1), (C.2), (C.3), and (C.4), the computer simulation numerically integrates $\dot{u}$, $\dot{v}$, $\dot{w}$, $\dot{p}$, $\dot{q}$, and $\dot{r}$ to obtain u, v, w, p, q, and r, respectively. The components of the spin of the sprung mass (i.e., p, q, and r) are used to solve for ϕ, θ, and ψ. The Euler angles (ϕ, θ, and ψ) and u, v, and w are used to solve for the inertial components (x, y, and z) of the location of the center of gravity of the sprung mass.

The following block diagram is intended to give a picture of the form of the computations described so far. The quantities calculated in Figure C.2 are used in determining forces and moments acting on the sprung and unsprung masses.

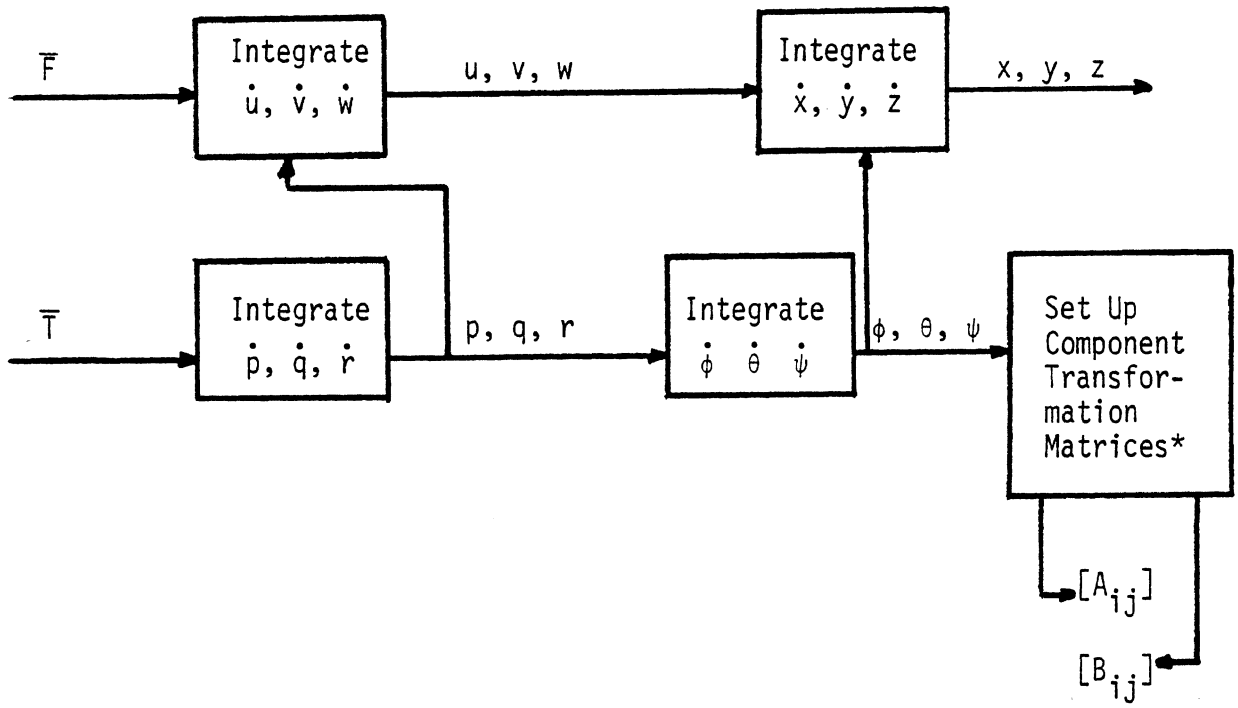

*Note: $[\hat{x}_b \hat{y}_b \hat{z}_b] = [\hat{x}_n \hat{y}_n \hat{z}_n]\,[A_{ij}]$

$[\hat{x}_b \hat{y}_b \hat{z}_b] = [\hat{x}_1 \hat{y}_1 \hat{z}_1]\,[B_{ij}]$

Figure C.2. Basic sprung mass motion calculations.

To calculate the suspension forces, the motions of points other than the center of mass are needed. Basic rigid body relations are used to compute the velocity of points of interest in the sprung mass from (1) the velocity of the mass center, (2) the spin of the body, and (3) the location of the point of interest with respect to the mass center.

Since the suspension forces are assumed in the model to act in a direction perpendicular to the road surface, the coordinate transformation matrix $[B_{ij}]$ (see Figure C.2) is employed as needed to express motions of points in the sprung mass with respect to the road axes.

C.3 Unsprung Mass Motions

The motions of the unsprung masses and the forces acting between the sprung and unsprung masses are treated by unique and unconventional methods in the model. It is not the purpose of this discussion to defend or criticize these techniques other than to note that they represent approximations which can be and have been confusing. The following discussion is intended to aid in understanding the approximations involved in the model.

In order to compute tire and suspension forces, the locations and velocities of the axles with respect to the sprung mass are calculated using the road axis system. (The road axis system may also be called the unsprung mass axis system.) Even though the center of the road axis system is taken to be below the center of mass of the sprung mass, the $\hat{x}_1$ and $\hat{y}_1$ components of any vector from the center of the road axis system to a particular point in the unsprung mass are assumed to be of fixed value. In addition, the spin of the road axis system is simply $\dot{\psi}\,\hat{z}_1$ (by definition of the road axis system). Consequently, the computation of the velocity or acceleration of any point in the unsprung mass is greatly simplified compared to the calculation of the general motion of a rigid body as expressed in a freely rotating coordinate system.

In practical terms, the assumptions described above state that the track and wheelbase remain constant when viewed from the $\hat{z}_1$ direction. However, the influences of the translational motions of the sprung mass center with respect to the tires have been omitted in the calculations of tire slip angles.

The lateral constraint between the sprung and unsprung masses is treated as a "horizontal" force in the $\hat{y}_1$ direction, acting at a given "roll center height" for each axle. The magnitude of this force is determined from the calculated values of the lateral forces produced by the tires and estimates of the lateral and yaw accelerations of the unsprung mass. For example, without going into detail, the estimated lateral acceleration of the front axle is given by the following equation:

$$\ddot{y}_f = (\dot{\overline{V}} \cdot \hat{y}_1) + x_u \ddot{\psi} \qquad (C.5)$$

where

$\ddot{y}_f$ is the lateral acceleration of the center of the front axle

$\dot{\overline{V}}$ is the acceleration of the sprung mass

x_u is the longitudinal distance from the unsprung mass center to the front axle

and $\ddot{\psi}$ is the yaw acceleration of the road axis (i.e., unsprung mass) system.

In simplified terms, the force of constraint between the front axle and the sprung mass is given by an equation of the following form:

$$F_{yc} = F_{y1} + F_{y2} - m_{uf}\ddot{y}_f \qquad (C.6)$$

where

F_{yc} is the force of constraint

F_{y1} is lateral force from the left-front tire

F_{y2} is lateral force from the right-front tire

m_{uf} is the mass of the front axle

$\ddot{y}_f$ is given by Equation (C.5)

Equations (C.5) and (C.6) are not the whole story, however. In the computer program "current" values of $\dot{\overline{V}}$ and $\ddot{\psi}$ are not available at the point in the computational sequence where F_{yc} would be evaluated. In fact, F_{yc} is being evaluated in order to evaluate $\dot{\overline{V}}$ and $\ddot{\psi}$. Rather than solving the appropriate equations simultaneously, estimates of $\dot{\overline{V}}$ and $\ddot{\psi}$ are used in computations of the form of (C.5) to estimate $\ddot{y}_f$. The quantities $\dot{\overline{V}}$ and $\ddot{\psi}$ are estimated from "current" values of the tire forces, the total mass of the unit, and the total yaw moment of inertia of the unit.

Calculations similar to the ones just described are carried out for each of the axles making up the unsprung masses.

It should be noted that the axles are allowed bounce and roll degrees of freedom in the $\hat{x}_1$ $\hat{y}_1$ $\hat{z}_1$ axis system.

The general idea of the method for computing axle motions is illustrated in Figure C.3.

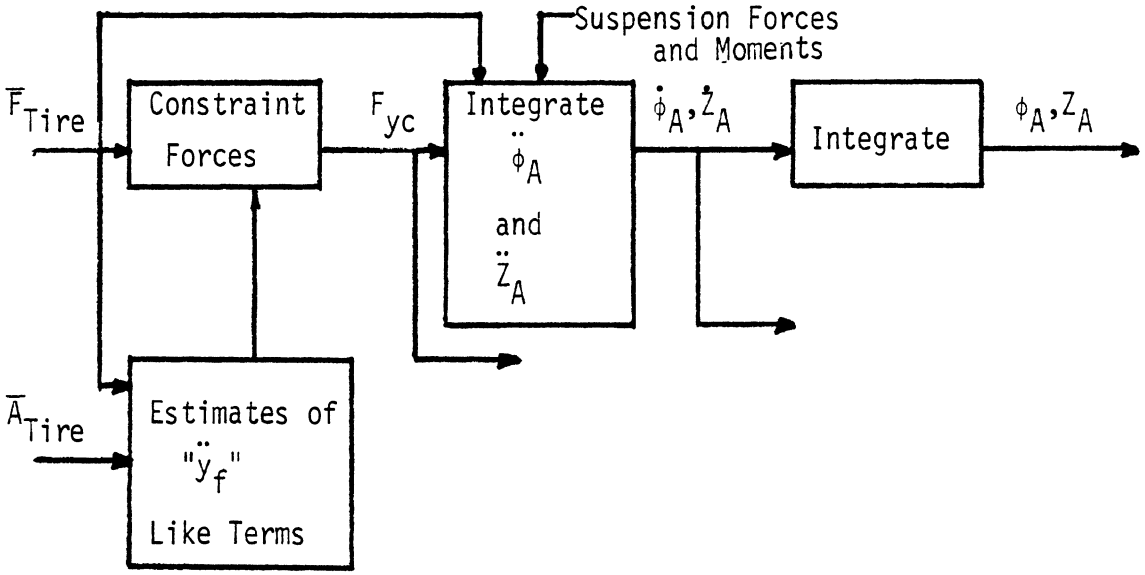

Figure C.3. Heuristic diagram for computation of axle motions.

C.4 Tire Forces and Moments

A semi-empirical tire model is used to fit tire data for use in the simulation. A recent description of the tire model is given in Reference [8]. The vertical load between the tire and road is computed from (1) the distance from the wheel center to the road plane in the $\hat{z}_1$ direction and (2) the time rate of change of that distance.

The lateral force from a tire is primarily a function of the tire's vertical load and slip angle. The slip angle for a tire is given by

$$\alpha_i = \tan^{-1}\left(\frac{v_i}{u_i}\right) - \delta_i \qquad (C.7)$$

where

α_i is the slip angle

v_i is the lateral velocity in the $\hat{y}_i$ direction of the wheel center

u_i is the longitudinal velocity in the $\hat{x}_i$ direction of the wheel center

and δ_i is the steer angle of the wheel if it has one.

The velocity components v_i and u_i of the wheel center in the $\hat{y}_i$ and $\hat{x}_i$ directions, respectively, are:

$$v_i = (\overline{V} \cdot \hat{y}_i) + \dot{\psi} x_i \qquad (C.8)$$

and

$$u_i = (\overline{V} \cdot \hat{x}_i) - \dot{\psi} y_i \qquad (C.9)$$

where x_i is the distance from the center of the unsprung mass axis system to the i^{th} axle and y_i is one-half of the track of the axle. (The signs of x_i and y_i are chosen appropriately for the location of the wheel involved.)

Tire aligning moment is computed using slip angle and vertical load in a table look-up routine.

C.5 Suspension Forces and Moments

Suspension forces are assumed to act in the $\hat{z}_1$ direction, which is normal to the road surface. Changes from the static equilibrium values of the spring forces on a level road are computed in the program. The values of these changes are based on empirical functions of the changes in the "vertical" ($\hat{z}_1$ direction) component of spring deflection and the time rates of change of the vertical components of spring deflection.

The program contains provision for interaxle load transfer in tandem suspensions during braking maneuvers, but this effect is not important in this study of turning without braking.

Auxiliary roll stiffnesses are included in the model to produce moments which usually oppose increases in the roll angle of the sprung mass with respect to an axle. These moments are in addition to those produced by the springs.

With regard to roll moments acting on the sprung mass, the suspension forces receive special treatment in the model. Figure C.4 illustrates the manner in which the moments about an axis in the $\hat{x}_1$ direction through the sprung mass center are computed in the simulation. Note that the "lever arms" for the suspension forces (SF1 and SF2) and the force of constraint (F_{yc}) changes as the roll angle (ϕ) of the sprung mass changes.

Using the approximation that ($h \sin \phi(SF2) + h \sin \phi(SF1)$) is approximately equal to $W_s h \sin \phi$, Equation (C.10), shown in Figure C.4, may be reduced to the form

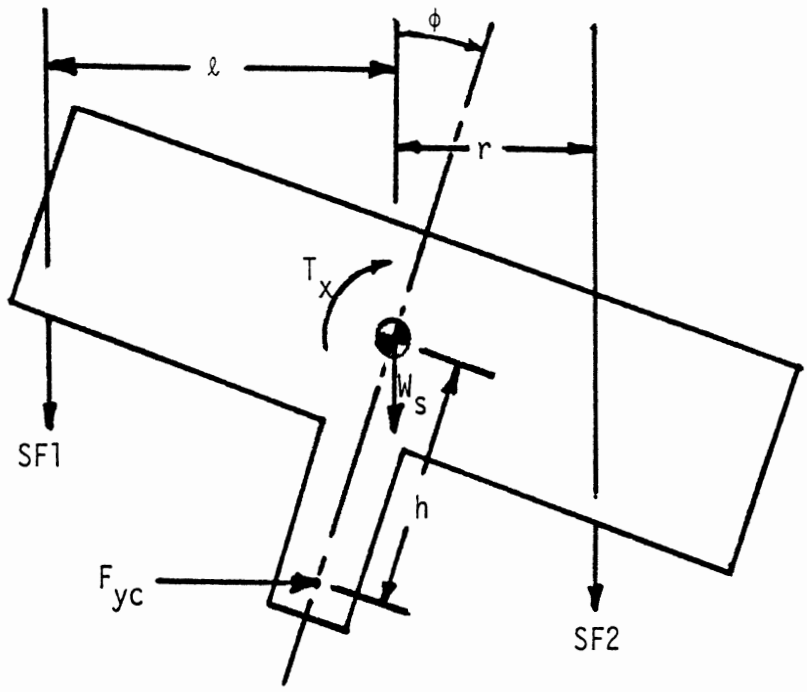

$$T_x = (SF2)r - (SF1)\ell - F_{yc}(h) \cdot (\cos \phi) \qquad (C.10)$$

Where

T_x is the moment about the $\hat{x}_1$ axis,

T is the distance between spring connections on the axle involved,

$r = T/2 - h \sin \phi$

$\ell = T/2 + h \sin \phi$

Figure C.4. Sprung mass roll moment.

$$T_x = (SF2 - SF1)T/2 - W_s h \sin \phi - F_{yc} h \qquad (C.11)$$

where $\cos \phi \doteq 1.0$.

In the simulation model, the forces and moments acting on the sprung mass are expressed in the $\hat{x}_1\ \hat{y}_1\ \hat{z}_1$ system and then transformed to the $\hat{x}_b\ \hat{y}_b\ \hat{z}_b$ system. This procedure was followed for convenience sake when the program was first written.

C.6 Gravitational Forces and the Inclined Road

Initially, the computer program was written with a flat, level road in mind. The suspension forces computed were actually the changes in suspension forces from the static forces needed to support the sprung mass. A similar idea was applied to the tire vertical force characteristics. Using this approach, the sprung and unsprung masses were automatically at their equilibrium positions at the start of a calculation on a level road. Furthermore, the influence of gravitational forces could be omitted from the dynamic calculations.

When an inclined road capability was added to the simulation, the gravitational forces did not have to be perpendicular to the road surface. The direction of the gravity vector was specified as follows:

$$\hat{g} = g_1 \hat{x}_n + g_2 \hat{y}_n + g_3 \hat{z}_n$$

where $\hat{g}$ is a unit vector in the direction of the gravitational acceleration, and

g_1, g_2, and g_3 are the direction cosines of $\hat{g}$ in the inertial axis system.

Since the inertial and road (or unsprung mass) system differ only by the heading angle, ψ, a single rotation can be used to express the gravitational direction vector, $\hat{g}$, in the unsprung mass coordinate system, viz.:

$$\hat{g} = \underline{|\hat{x}_n \; \hat{y}_n \; \hat{z}_n|} \begin{bmatrix} g_1 \\ g_2 \\ g_3 \end{bmatrix}$$

$$= \underline{|\hat{x}_1 \; \hat{y}_1 \; \hat{z}_1|} \begin{bmatrix} (\cos\psi)g_1 + (\sin\psi)g_2 \\ (-\sin\psi)g_1 + (\cos\psi)g_2 \\ g_3 \end{bmatrix}$$

The inclined road discussions given in [4] on pages 51-53 and [8] on pages 124-127 are for a unit vehicle. Arguments similar to those used in [4] and [8] can be applied to an articulated vehicle. The following discussion is intended to aid in understanding the inclined road representation in the simulation of an articulated vehicle.

In the level road case, the static levels of the spring forces "cancel" the gravitational forces from the individual masses. This idea may be expressed in equations as follows using the tractor sprung mass as an example.

$$m\ddot{z} = F_{sus} + W_s + (\overline{F}_5 \cdot \hat{z}_n) \qquad (C.12)$$

where

$F_{sus} = F_{suso} + \Delta F_{sus}$ (total suspension force)

W_s = weight of the sprung mass

$\overline{F}_5 = F_{50}\hat{z}_n + \Delta\overline{F}_5$ (total 5th wheel force)

and

$$F_{suso} + F_{50} + W_s = 0 \qquad (C.13)$$

or (for a level road)

$$m\ddot{z} = \Delta F_{sus} + (\Delta\overline{F}_5 \cdot \hat{z}_n) \qquad (C.14)$$

Hence, in the computer program ΔF_{sus} and $\Delta \bar{F}_5$ are computed. The initial conditions of the sprung and unsprung masses are then the static equilibrium positions on a level road.

To avoid modifying the simulation to any great extent, the same initial conditions as were used in the level road case are used for computing motion on an inclined road; however, the vehicle is not initially in static equilibrium on an inclined road. Furthermore, modifications of the force equations must be considered in three directions, not just in the vertical direction, viz.,

$$m\dot{\bar{V}} = \bar{F}_{sus} + W_s(g_1\hat{x}_n + g_2\hat{y}_n + g_3\hat{z}_n) + \bar{F}_5$$

where

$$\bar{F}_{sus} = \Delta\bar{F}_{sus} + F_{suso}\,\hat{z}_n$$

$$\bar{F}_5 = \Delta\bar{F}_5 + F_{50}\,\hat{z}_n$$

and (as before)

$$F_{suso} + F_{50} + W_s = 0$$

or (for an inclined road)

$$m\dot{\bar{V}} = \Delta\bar{F}_{sus} + F_{suso}\,\hat{z}_n + W_s(g_1\hat{x}_n + g_2\hat{y}_n + g_3\hat{z}_n) + \Delta\bar{F}_5 + F_{50}\,\hat{z}_n \qquad (C.15)$$

To use the quantities ΔF_{sus} and $\Delta \bar{F}_5$ as they were used for a level road, it is convenient to rewrite (C.15) as follows:

$$m\dot{\bar{V}} = \Delta\bar{F}_{sus} + \Delta\bar{F}_5 + W_s(g_1\hat{x}_n + g_2\hat{y}_n + g_3\hat{z}_n) + (F_{suso} + F_{50} + W_s)\hat{z}_n - W_s\,\hat{z}_n$$

But $F_{suso} + F_{50} + W_s = 0$, hence

$$m\dot{\overline{V}} = \Delta\overline{F}_{sus} + \Delta\overline{F}_5 + W_s(g_1\hat{x}_n + g_2\hat{y}_n + (g_3-1)\hat{z}_n) \qquad (C.16)$$

Equation (C.16) indicates that the influence of an inclined road may be included into the calculation procedure used for a level road by adding a force acting at the sprung mass center equal to $W_s(g_1\hat{x}_n + g_2\hat{y}_n + (g_3-1)\hat{z}_n)$.

A procedure similar to the one discussed above is employed at each mass center in the vehicle system when the inclined road option is used. Static loads for a level road are computed and printed out at the beginning of all simulation runs.

C.7 Torsional Compliance in the Frames and Fifth Wheel

The simulation model has been modified to treat torsional roll compliance in the frames of the tractor and semitrailer. These modifications are discussed in Appendix D. Prior to the modification, all roll coupling between the tractor and the semitrailer was lumped into a so-called "fifth-wheel compliance."

APPENDIX D

A MODIFICATION FOR TORSIONALLY-COMPLIANT TRACTOR AND SEMITRAILER FRAMES

The Phase II articulated vehicle simulation used a "roll-spring" between the tractor and trailer to approximate the effects of fifth wheel compliance.* A schematic diagram of this model is shown in Figure D.1. The desire to more accurately model lateral load transfer has led to the addition of the torsionally-compliant tractor as well.

A sketch of the modified tractor-trailer combination, with the tractor and the trailer assumed to be flexible in roll with stiffnesses XTT and TRSTF, respectively, is shown in Figure D.2. The roll angle of the tractor is Y(19), that of the trailer is Y(31). In addition, the roll angle of the massless fifth wheel is defined as Y45.

Figure D.3 shows the forces and moments acting on the rear area of the tractor sprung mass. Note it has been assumed that the torsionally-compliant element is midway between the hitch force, PINY, and the lateral force, SMY. Thus, since in the nomenclature of the computer program PINY is D above the c.g. and SMY is FRZ below the c.g., we have

$$Q = \frac{D + FRZ}{2} \tag{D.1}$$

Now the requirement for equilibrium of the massless hitch yields

$$TP + (PINY-SMY)Q + KRS(\theta_{axle} - Y45) + M_{SF} + XTT(Y(19) - Y45) = 0 \tag{D.2}$$

where KRS is the auxiliary roll stiffness, θ_{axle} is the roll angle of the axle, M_{SF} is the moment applied by the suspension forces, SF, and TP is the roll moment acting on the tractor coming from the trailer.

---

*See the Phase II Technical Report [4], pp. 48-50 and 73-78.

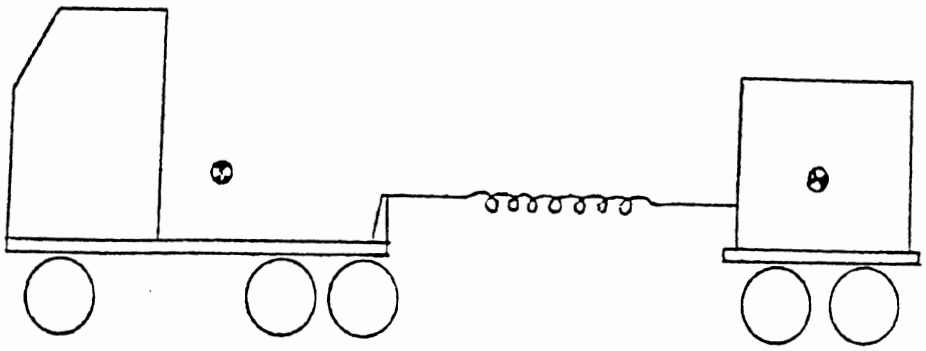

Figure D.1

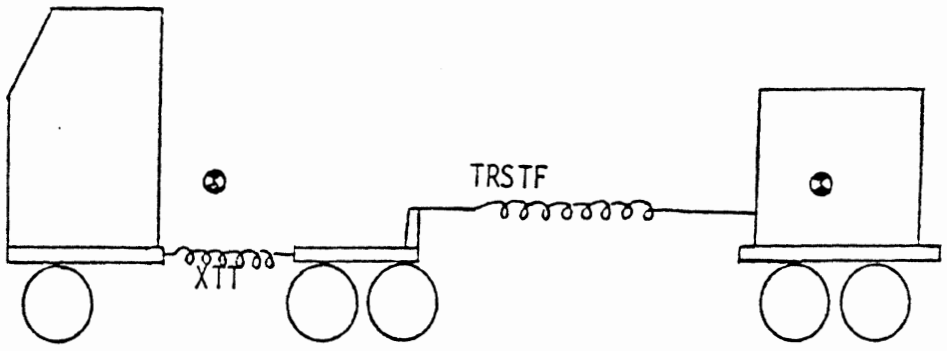

Figure D.2

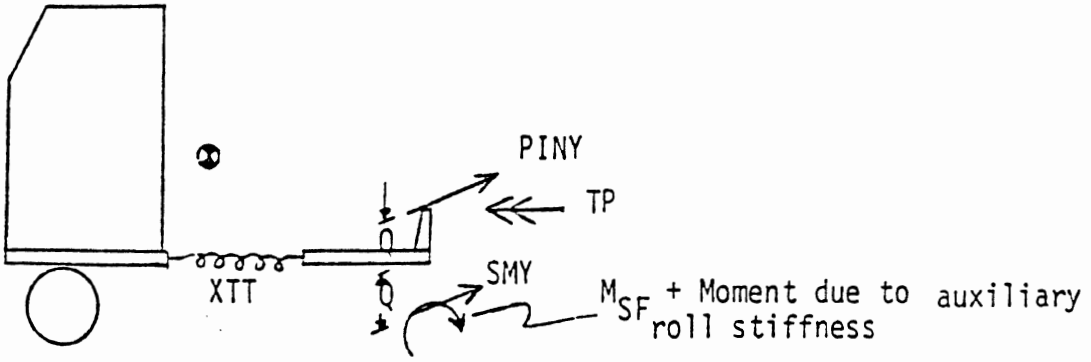

Figure D.3

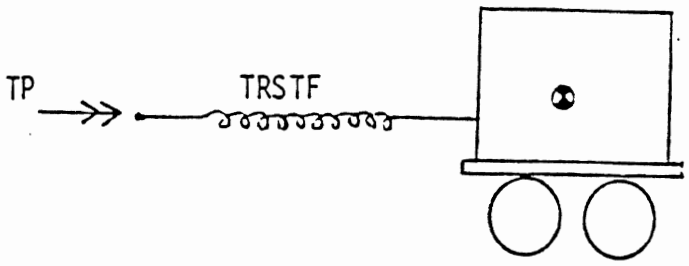

Figure D.4

Moment equilibrium of the massless torsional trailer element of Figure D.4 yields

$$-TP - TRSTF(Y45 - Y(31)) = 0 \qquad (D.3)$$

TP can be eliminated from Equations (D.2) and (D.3) to solve for Y45.

$$Y45 = [XTT\ Y(19) + M_{SF} + KRS\ \theta_{axle} + TRSTF\ Y(31) + (PINY-SMY)Q]/(XTT + TRSTF + KRS) \qquad (D.4)$$

Equation (D.4) is used in subroutine FCT to compute Y45. Y45, in turn, is used to locate the frame rails for the calculation of suspension forces and moments. Further, Equation (D.3) yields TP which is a roll couple applied to the tractor and trailer. In the equations of motion in the simulation, TP replaces the moment formerly associated with the "roll-spring" of Figure D.1.

Throughout the discussion above, the spring rates have been treated as linear. However, in the program the springs may be non-linear (and, in fact, can be "springs with friction"). For nonlinear springs, the "local linearized spring rates" are computed and used in Equations (D.3) and (D.4).

APPENDIX E

TRACTOR-SEMITRAILER STEADY TURNING RESPONSE

The purpose of this discussion is to communicate pertinent technical matters which can be used to evaluate and interpret results (either measured or simulated) for tractor-semitrailer vehicles performing constant velocity turns. A simple model will be employed in the ensuing discussion to illustrate a number of useful ideas. The form of the model employed in this appendix might be described as a "three-wheel bicycle model." In this model there are three lateral forces acting on the vehicle at three suspension reference points. Each of these lateral forces represents the total tire force generated by all the tires on any axle (or set of axles if the vehicle is equipped with tandem suspensions).

For a steady turn, the "three-wheel bicycle model" appears as shown in Figure E.1 below. For the small angles attained in typical

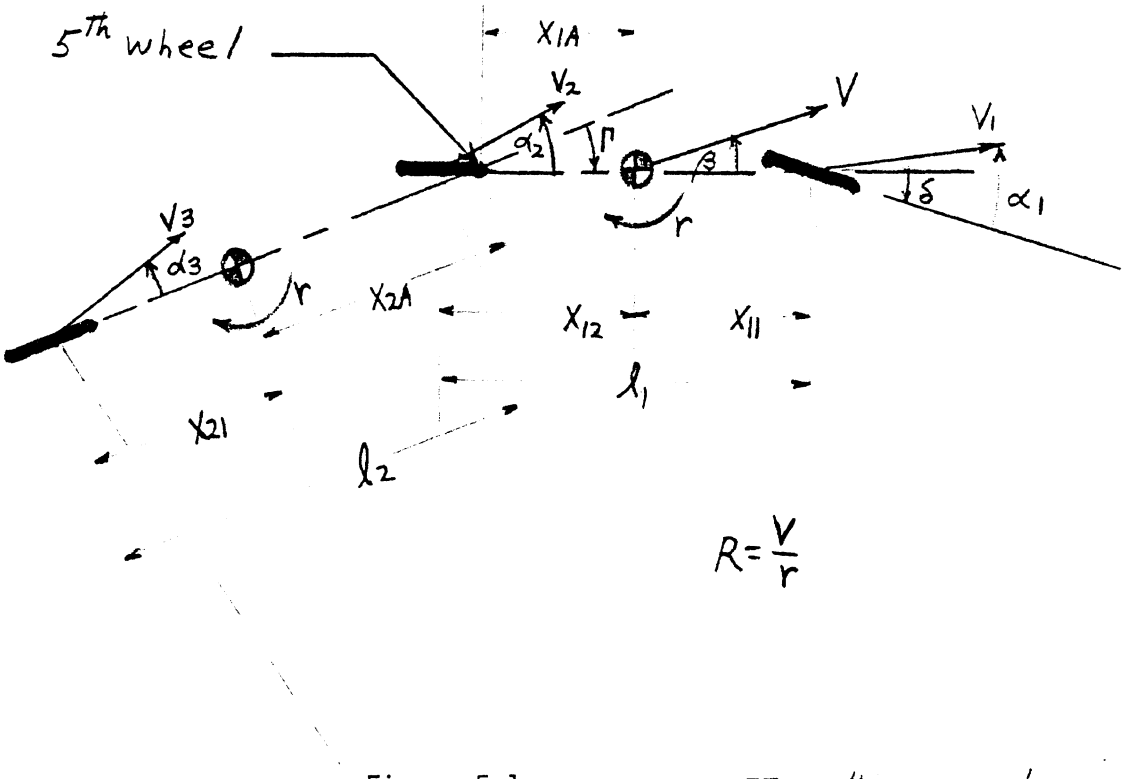

Figure E.1

maneuvers at highway speeds

$$\alpha_1 \doteq \beta - \delta + x_{11}\, r/V \tag{E.1}$$

$$\alpha_2 \doteq \beta - x_{12}\, r/V \tag{E.2}$$

$$\alpha_3 \doteq \beta + \Gamma - (x_{1A} + x_{2A} + x_{21})r/V \tag{E.3}$$

$$\delta = \alpha_2 - \alpha_1 + \ell_1\, r/V \quad \text{where } \ell_1 = \text{tractor wheelbase} \tag{E.4}$$

$$\Gamma = \alpha_3 - \alpha_2 + \ell_2\, r/V \quad \text{where } \ell_2 = \text{wheelbase between last two axles} \tag{E.5}$$

For a steady turn it can also be shown that the lateral and vertical forces satisfy the following relationships*:

$$\frac{F_{y_1}}{F_{z_1}} = \frac{A_y}{g} = \frac{F_{y_2}}{F_{z_2}} = \frac{F_{y_3}}{F_{z_3}} \tag{E.6}$$

In the linear range, tire lateral forces are related to their slip angles by their cornering stiffnesses, viz.:

$$F_{y_i} = - C_{\alpha_i} \alpha_i \tag{E.7}$$

where C_{α_i} is the total cornering stiffness for all the tires on the i^{th} suspension.

Thus, combining (E.4), (E.5), (E.6), and (E.7) yields:

---

*These relationships can be verified by envisioning the similarity of the force diagrams for a side view (gravitational forces) and a top view (lateral d'Alembert forces for a steady turn) of a tractor-semitrailer vehicle.

$$\delta = \left(- \frac{F_{z_2}}{C_{\alpha_2}} + \frac{F_{z_1}}{C_{\alpha_1}} \right) \frac{V^2}{Rg} + \frac{\ell_1}{R} \qquad \text{(E.8)}$$

and

$$\Gamma = \left(- \frac{F_{z_3}}{C_{\alpha_3}} + \frac{F_{z_2}}{C_{\alpha_2}} \right) \frac{V^2}{Rg} + \frac{\ell_2}{R} \qquad \text{(E.9)}$$

and, consequently, the articulation gain is given by:

$$\frac{\Gamma}{\delta} = \frac{\left(\frac{F_{z_2}}{C_{\alpha_2}} - \frac{F_{z_3}}{C_{\alpha_3}} \right) \frac{V^2}{g} + \ell_2}{\left(\frac{F_{z_1}}{C_{\alpha_1}} - \frac{F_{z_2}}{C_{\alpha_2}} \right) \frac{V^2}{g} + \ell_1} \qquad \text{(E.10)}$$

The quantities

$$D_1 = F_{z_1}/C_{\alpha_1}$$

$$D_2 = F_{z_2}/C_{\alpha_2}$$

$$D_3 = F_{z_3}/C_{\alpha_3}$$

are called the "cornering compliances." The difference between "front and rear" cornering compliances for the tractor and the trailer determine the influence of lateral acceleration on the steer and articulation angles required for a specified turn.

Using

$$K_1 = D_1 - D_2 \qquad \text{(E.11)}$$

and equivalence between the steer angle equation for a tractor and a straight truck can be noted, viz.:

$$\delta = K_1 \frac{V^2}{Rg} + \frac{\ell_1}{R}$$ where K_1 is called the understeer factor for either a straight truck or tractor of an articulated vehicle. (E.12)

It is also interesting to note similarities between the trailer and tractor equations. (A physical understanding of these similarities can be obtained by thinking of the tractor's rear wheels as the "steered wheels" for the trailer.) If a "trailer understeer factor" is defined as follows:

$$K_2 = D_2 - D_3 \tag{E.13}$$

then

$$\Gamma = K_2 \frac{V^2}{Rg} + \frac{\ell_2}{R} \tag{E.14}$$

Based on Equations (E.12) and (E.14), the steady turning performance of a tractor-semitrailer vehicle could be quantified by two experimentally determined parameters, namely, K_1 and K_2.

Nevertheless, a more comprehensive analysis shows that for vehicles with tandem axles the quantities ℓ_1 and ℓ_2 measured to points midway between the axles are approximately, but not exactly, correct [11]. The results of Reference [11] indicate, however, that the form of Equations (E.12) and (E.14) are appropriate and that four parameters (i.e., K_1, K_2, ℓ_{1e}, and ℓ_{2e}, where ℓ_{1e} and ℓ_{2e} are "effective wheelbases") need to be evaluated from test data in order to specify steady turning performance.

Theoretically, if velocity, yaw rate, articulation angle, and front-wheel steer angle were measured for two different steady turns, then the parameters K_1, K_2, ℓ_{1e}, and ℓ_{2e} could be evaluated using Equations (E.12) and (E.14) to solve for the values of these parameters. However, accurate measurement of front-wheel steer angle has proven to be difficult in practice. Certainly, it is easier to measure steering-wheel angle than front-wheel angle. Yet, due to (1) compliances and hysteresis in the steering system, (2) side-to-side differences in front-wheel angles, and (3) roll-steer effects, it is difficult to use steering-wheel angle to estimate front-wheel angle.

An approach, which has been used to avoid the difficulties associated with measuring properties and variables within the steering system, is to use a "reference front-wheel angle," which is simply the steering-wheel angle divided by the overall steering ratio. In this approach, K_1 includes the influences of steering compliance, roll steer, and other steering properties. Although proceeding in this fashion does avoid dependence upon measuring front-wheel angles, in practice, it still produces test data with non-negligible scatter from run to run.

Since (1) an equation of the form of (E.12) describes either a tractor or a straight truck and (2) the steady turning properties of the straight-truck version of the tractor used in this study have been investigated in a previous project [7], the properties of the articulation angle between tractor and trailer will be emphasized in the following discussion.*

Rewriting Equation (E.9) for articulation angle in terms of yaw rate, r, and velocity, V (that is, the quantities which have been measured in vehicle tests) yields:

$$\Gamma = \frac{\ell_2 r}{V} + (K_2)\,\frac{rV}{g} \qquad (E.15)$$

where

$$\left(\frac{F_{z_2}}{C_{\alpha_2}} - \frac{F_{z_3}}{C_{\alpha_3}}\right) = D_2 - D_3 = K_2$$

If $\frac{\ell_2 r}{V} >> (K_2 \frac{rV}{g})$, then Γ is nearly determined by the wheelbase, ℓ_2, and the radius, R, of the turn, i.e.,

$$\Gamma \simeq \ell_2/R \quad \text{radians}$$

*Also, it might be noted that investigating articulation angle avoids the necessity of accounting for the idiosyncracies of the steering system.

For example, if the tractor rear tires and the trailer tires are equally loaded and of identical lateral force characteristics, then $D_2 \doteq D_3$, $K_1 \doteq 0$, and $\Gamma \doteq \ell_2/R$. As a typical example in which tractor and trailer tires are not identical, assume that the following parametric values represent a reasonable situation.

Example Values:

$F_{z_2} = F_{z_3} = 32{,}000$ lbs

$C_{\alpha_2} = 8(600$ lbs/deg)

$C_{\alpha_3} = 8(500$ lbs/deg)

} assumes 8 tires on these suspensions

$V = 45$ mph (66 ft/sec)

$A_y = Vr = 0.25$

$\ell_2 = 34$ ft.

For the Example Values:

$r = 7°$/sec

$R = 541$ ft.

$D_2 = 6.67$ deg/g

$D_3 = 8.00$ deg/g

$K_2 = -1.3$ deg/g

$\Gamma = 3.27$ deg

(This situation could be referred to as "oversteer" since less than the zero speed angle of 3.6° is required.) Or, if the tractor tires are switched with the trailer tires, then

$$\Gamma = 3.93 \text{ deg}$$

In summary, these calculations indicate that the articulation angle is not expected to differ much from that determined by the wheelbase/turn radius influence for low severity maneuvers.

The following discussion goes into the details of investigating the steady turning behavior of an articulated vehicle based on an

analysis of articulation angle gain (that is, the ratio of articulation angle to front-wheel angle).

Let

$$A_G = \frac{\Gamma}{\delta} = \frac{\ell_2 + K_2 V^2}{\ell_1 + K_1 V^2} \qquad \text{(E.16)}$$

where positive Γ is defined as shown in the following sketch.

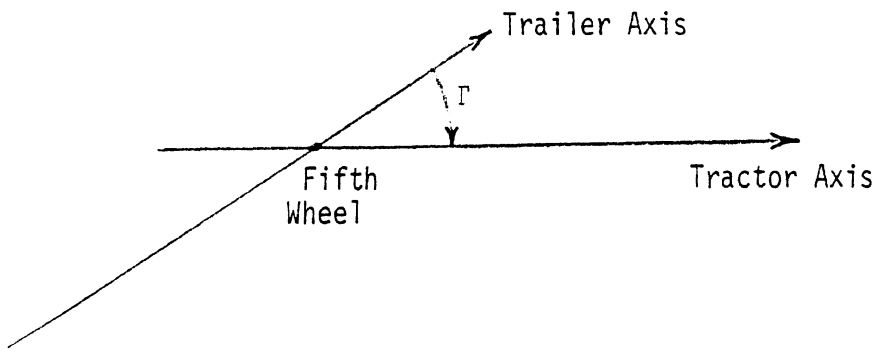

For tests at fixed steering-wheel angle and gradually increasing velocity $A_G \doteq \ell_2/\ell_1$ for $V \approx 0$. At least mathematically, for $\ell_2 << |K_2|V^2$ and $\ell_1 << |K_1|V^2$, $A_G \to K_2/K_1$ as $V \to \infty$. The gain "blows up" (i.e., $A_G \to \pm\infty$) for $K_1 < 0$ and $\ell_1 + K_1 V^2 \approx 0$. Several types of graphs of A_G versus V^2 are possible, depending upon the values of K_1, K_2, ℓ_1, and ℓ_2, viz.:

1) for $K_1 > 0$ and $K_2 > 0$

Case 1:

$K_2 > K_1\ell_2/\ell_1$

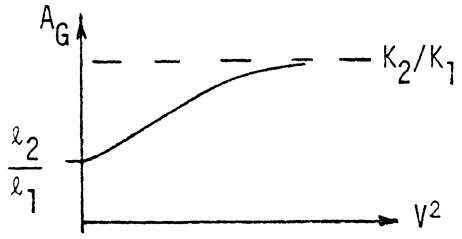

and

Case 2:

$K_2 < K_1\ell_2/\ell_1$

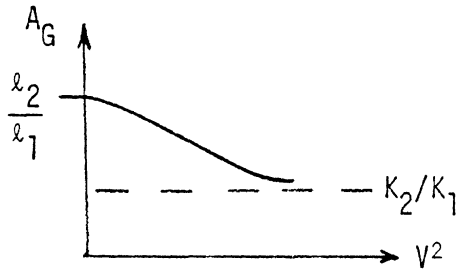

2) for $K_1 < 0$ and $K_2 > 0$

V_{cr} = critical speed for the tractor i.e., $\ell_1 + K_1 V_{cr}^2 = 0$

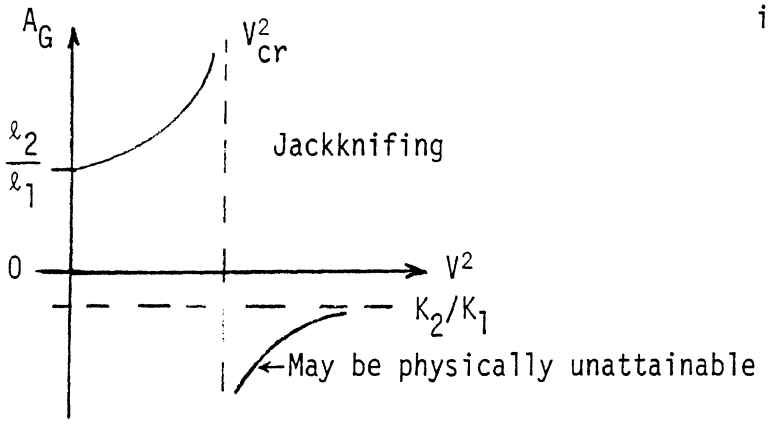

3) for $K_1 > 0$ and $K_2 < 0$

V_o = speed at which articulation angle equals zero, i.e., $\ell_2 + K_2 V_o^2 = 0$

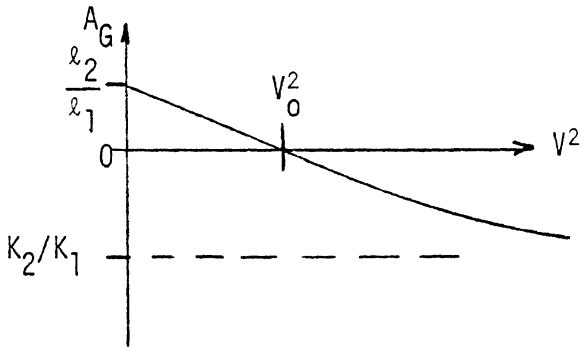

4) for $K_1 < 0$ and $K_2 < 0$

Case 1:

$K_2 > K_1 \ell_2 / \ell_1$

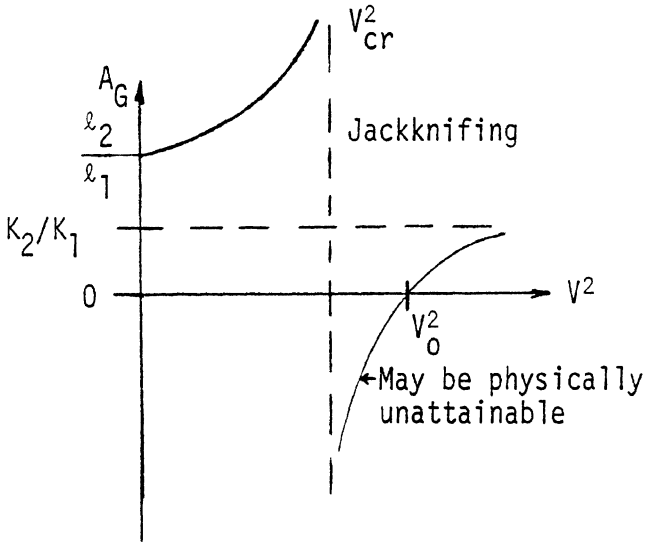

V_{cr} = critical speed for the tractor

V_o = speed at which articulation angle equals zero

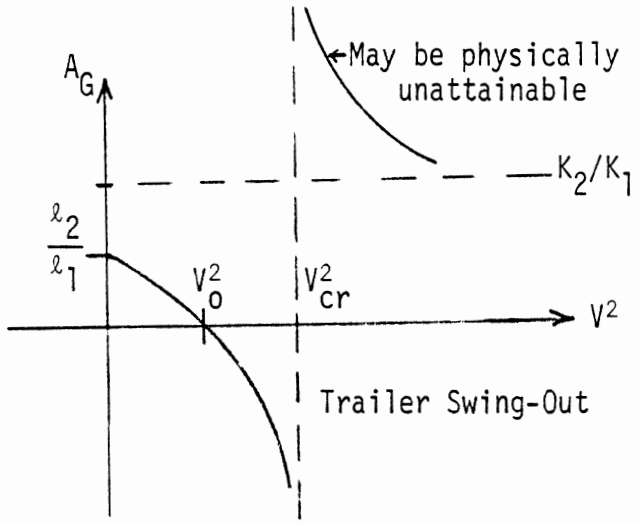

Case 2:

$K_2 < K_1\ell_2/\ell_1$

Note that the qualitative graphs for cases 1 and 2 for $K_1 < 0$ and $K_2 < 0$ are deduced as follows:

$$\frac{\partial A_G}{\partial V^2} = \frac{K_2\ell_1 - K_1\ell_2}{(\ell_1 + K_1V^2)^2} \tag{E.17}$$

$$\frac{\partial A_G}{\partial V^2} > 0 \quad \text{if} \quad K_2 > K_1\ell_2/\ell_1 \tag{E.18}$$

(Note that (E.18) is true at all velocities except V_{cr}.)

and $$\frac{\partial A_G}{\partial V^2} < 0 \quad \text{if} \quad K_2 < K_1\ell_2/\ell_1 \tag{E.19}$$

In order that (1) the slopes have the appropriate signs and (2) the curves go to infinity with the right polarity at V_{cr}, the graphs must have the qualitative shapes shown here.

It seems intuitively correct to define (a) cases in which A_G goes to $-\infty$ at V_{cr} as "trailer swing-out" and (b) cases in which A_G goes to $+\infty$ at V_{cr} as "jackknifing," because in (a) the trailer is swinging outside the turn and in (b) the vehicle is folding up on the inside of the turn. Note that the tractor portion must be oversteer

for either unlimited jackknifing or unlimited trailer swing-out to occur. For unlimited trailer swing-out to occur, V_o must be less than V_{cr}.